[redacted]
TOP SECRET
NO FOREIGN DISSEMINATION

[redacted]
14 000391170

Total No. of Pages 78
Copy No. [redacted] of [redacted] Copies

PERFORMANCE ANALYSIS FOR THE 1103 SYSTEM

20 DECEMBER 1968

CONTRIBUTORS: [redacted]

Itek OPTICAL SYSTEMS DIVISION
ITEK CORPORATION • 10 MAGUIRE ROAD • LEXINGTON, MASSACHUSETTS 02173

[redacted]

TOP SECRET
NO FOREIGN DISSEMINATION

HANDLE VIA
TALENT-KEYHOLE
CONTROL SYSTEM ONLY

CONTENTS

1. Summary 1-1

2. Analysis of Focus Problem 2-1
   2.1 Air-To-Vacuum Focus Shift 2-1
   2.2 Optimum Focus for Aerial Photography 2-3

3. System Performance 3-1
   3.1 CORN Target Resolution 3-1
   3.2 Determination of Operational Resolution 3-3
   3.3 Comparison of CORN Target and Predicted Resolutions 3-9
   3.4 Evaluation of System Operation 3-10

4. A-Takeup Experiment 4-1
   4.1 General 4-1
   4.2 Resolution as a Function of Contrast 4-1
   4.3 Granularity as a Function of Density 4-6
   4.4 Modulation Transfer as a Function of Spatial Frequency 4-7
   4.5 Comparing the Three Image Quality Parameters 4-10

5. Density Analysis 5-1
   5.1 Objective 5-1
   5.2 Procedure 5-1
   5.3 Results 5-5

6. Recommendations 6-1

Appendices

   A Resolution Predictions for CORN Targets A-1
   B Resolution Predictions for HPL Targets B-1
   C Photographic Illustrations C-1
   D Weather Assessment D-1
   E Analysis of DRT Photographic Tests on System 1109 . . . . . E-1
   F Special Resolution Tests on System 1105 . . . . . F-1

FIGURES

3-1 Dynamic Resolution Versus Focus Position, AFT-Looking Camera No. 306, Along Track 3-5
3-2 Dynamic Resolution Versus Focus Position, AFT-Looking Camera No. 306, Cross Track 3-6
3-3 Dynamic Resolution Versus Focus Position, FWD-Looking Camera No. 307, Along Track 3-7
3-4 Dynamic Resolution Versus Focus Position, FWD-Looking Camera No. 307, Cross Track 3-8
3-5 Altitude Distribution of HPL Targets 3-11
4-1 Structure of the A-Takeup Experiment 4-2
4-2 Object Target Modulation Versus Recorded Target Resolution for Mission 1103 (Horizontal Bars Represent Real Data Contained Within 95-Percent Confidence Limits) 4-4
4-3 Resolution as a Function of Contrast for Each of the Three Film Conditions on Each of the Three J-3 Mission A-Takeup Experiments 4-5
4-4 Granularity as a Function of Density 4-6
4-5 Comparison of the Sharpest and Broadest Smoothed Edges (All of the Nine Edges Constituting the Base Data for this MTF Analysis are Contained Within These Limits.) 4-8
4-6 Average MTF's (Solid Lines) for Each of the Three Test Conditions With Respective Experimental Variation (Dashed Lines) 4-9
4-7 Average MTF's for 1101, 1102, and 1103 Missions 4-11
E-1 Comparative Dynamic Resolution Through-Focus Tests on Unit No. 316 . . . . . E-2
E-2 Comparative Dynamic Resolution Through-Focus Tests on Unit No. 317 . . . . . E-3
E-3 Dynamic Resolution Through-Focus Tests on Instrument No. 317 for Different Values of IMC Mismatch E-5
F-1 Unit No. 310, Low Contrast Resolution Readings F-1
F-2 Unit No. 311, Low Contrast Resolution Readings F-2
F-3 Unit No. 311, High Contrast Resolution Readings F-3

TABLES

3-1 CORN Target Coverage 3-1
3-2 Resolution Target Readings, Average of Two Readers 3-2
3-3 Mission 1103 Exponents 3-4
3-4 CORN Target Readings and Predictions 3-9
3-5 List of System Configurations 3-13
3-6 Comparative Chart of Average System Performance, Low Contrast GRD 3-13
4-1 Results of 1103 Resolution Data Reduction 4-3
4-2 RMS Granularity at 1.0 Gross Density 4-7
5-1 Density Analysis of Mission 1103. 5-2
5-2 Eastman Kodak Terrain Densities 5-6
5-3 Average Target Density Values Calculated From Table 5-1 5-6
5-4 Filter Comparison With Regard to Target ΔD 5-7
A-1 Resolution Predictions for CORN Targets, FWD-Looking Camera, Unit No. 307 . . A-2
A-2 Resolution Predictions for CORN Targets, AFT-Looking Camera, Unit No. 306 . . A-3
B-1 Resolution Predictions for HPL Targets, FWD-Looking Camera, Unit No. 307 . . B-1
B-2 Resolution Predictions for HPL Targets, AFT-Looking Camera, Unit No. 306 . . B-7
B-3 Average Low Contrast Ground Resolved Distance Versus Photointerpreter Ratings . B-9
C-1 Ephemeral Information for the MIP Frames Under Consideration. C-1
D-1 Weather Estimate Averages for the Entire Panoramic Coverage Portion of the Mission D-1
D-2 Weather Estimate Mission 1103-1 . . . . . D-2
D-3 Comparison of Final Averages Obtained From Missions 1101, 1102 and 1103 . . . D-3

1. SUMMARY

The performance of the 1103 system was different than the performance of either the 1101 or the 1102 system. The best description of the 1103 system performance as evidenced in the photographic record can be found in the PEIR Report* on mission 1103, several sections of which are quoted below:

> "THE PET JUDGED THE GENERAL IMAGE QUALITY OF MISSION 1103 AS FAIR, AND NOT AS GOOD AS MISSION 1102. THERE WAS A SIGNIFICANT VARIABILITY IN IMAGE QUALITY THAT WAS GREATER THAN NORMALLY ENCOUNTERED WITH A KH-4B SYSTEM. THIS VARIABILITY RANGES FROM RATHER GOOD TO POOR. THE PHOTOINTERPRETERS REPORTED THAT 'THE INTERPRETABILITY OF THE IMAGERY ON THIS MISSION IS CONSIDERED TO BE MORE VARIABLE THAN THE IMAGERY OBTAINED ON MISSIONS 1101 AND 1102. IN ADDITION THE IMAGERY OF THE FORWARD-LOOKING CAMERA RECORD IS SUPERIOR TO THAT OF THE AFT CAMERA IN ALMOST EVERY CASE. THE OVERALL MISSION INTERPRETABILITY IS RATED AS FAIR.' THE EXACT CAUSE OF THE VARIABILITY IS NOT CLEAR; MAJOR FACTORS, HOWEVER, APPEAR TO BE HAZE AND FOCUS. THIS MISSION WAS SEVERELY AFFECTED BY HAZE, BUT IT CANNOT BE POSITIVELY STATED THAT WEATHER WAS THE MAJOR CAUSE OF THE QUALITY VARIATION. THE GENERAL QUALITY OF THE AFT-LOOKING RECORD IS LESS THAN THAT OF THE FORWARD-LOOKING. IN GENERAL, THE AFT-LOOKING RECORD APPEARS TO HAVE SLIGHTLY SOFTER FOCUS. ALTHOUGH THERE IS SOME EVIDENCE OF BETTER AFT-LOOKING IMAGERY ON THE VERY FIRST PORTIONS OF THE MISSION, AFT-LOOKING IMAGERY COMPARABLE TO THAT OF THE EARLY PORTIONS IS NOT EVIDENCED LATER IN THE MISSION, EVEN WHEN FAVORABLE WEATHER CONDITIONS EXISTED. . . . .THERE IS EVIDENCE THAT AT LEAST A PORTION OF THE DEGRADATION IN OVERALL MISSION QUALITY IS DUE TO IMAGE SMEAR. THIS CONDITION IS APPARENT ON FRAMES WHERE THE MAXIMUM SLIT WIDTH WAS USED. FOCUS VARIABILITY APPEARS TO HAVE BEEN THE MAJOR CAUSE OF IMAGE DEGRADATION. HOWEVER, SEVERE HAZE, THERMAL GRADIENTS, FOCUS AND SMEAR OFTEN COMBINED TO PRODUCE IMAGERY POORER THAN THAT ATTRIBUTABLE TO FOCUS ALONE. ALSO, IN SOME CASES, THESE FACTORS APPEARED TO BE COMBINED IN SUCH A MANNER AS TO PRODUCE GOOD IMAGERY. THE ULTIMATE CAPABILITY OF THE MISSION 1103 CAMERA SYSTEM IS INDICATED BY THE RESOLUTION LEVEL

[redacted]

AND FROM GROUND TARGETS. THE CORN* MOBILE TARGETS WERE THE BEST YET RECORDED, PRODUCING EIGHT FOOT GRD†, WHEREAS THE BEST FIXED TARGET PRODUCED SIX FEET GRD. THESE READINGS ARE INDICATIVE, HOWEVER, ONLY OF BEST PERFORMANCE AND NOT GENERAL PERFORMANCE."

The contractor's independent evaluation of the photographic record of mission 1103, conducted mainly on dupe positive materials, reached the following conclusions:

1. Image quality of the 1103 system for geographical areas known to have dry climates and low moisture content in the atmosphere (for example deserts) is obviously superior to the system image quality for areas with an appreciable amount of moisture in the atmosphere (haze but no cloud cover). The haze is quite obvious when examining the terrain camera (DISIC) photography and comparing the images of the FWD- and AFT-looking cameras of the same ground objects. The degradation in performance over the hazy areas should be attributed mainly to weather and atmospheric conditions. True indications of the system's potential performance can best be determined by evaluating the system's photography over deserts or geographic areas known to have dry climates. Conclusions can then be arrived at by combining these data with known anomalies in the system's operation during the mission.

2. The performance of the FWD-looking camera was better than that of the AFT-looking camera throughout the mission, but the difference in performance between the two cameras was very marked over areas where haze prevailed. Thus, the difference in performance over the hazy areas should be attributed mainly to the different filters that were utilized (a W-25 in the FWD-looking camera and a W-21 or SF-05 in the AFT-looking camera).

3. In the AFT-looking camera, the SF-05 filter was used extensively. This filter produces very low contrast imagery especially in the presence of haze. Twenty-one HPL‡ targets were assigned to the SF-05 filter; however, due to programmer limitations, 39 percent of the total photographic record of the AFT-looking camera was taken with the SF-05 filter, and, perhaps more significantly, approximately 67 percent of the HPL targets photographed by the AFT-looking camera were exposed through the SF-05 filter. It is the contractor's opinion that the AFT-looking camera's rating has been adversely affected by the extensive use of the SF-05 filter.

4. From the photographic record, it appears that the contrast of the AFT-looking camera would have been improved if a W-25 filter were used instead of the W-21 over areas covered with haze. Similarly, it seems that the performance of the FWD-looking camera would have been improved if a W-21 filter were used over desert areas. (It seems that the FWD-looking camera's photography was lacking in grey tones over desert areas.)

The following conclusions have been reached as described in the various sections of the report:

1. Section 2.1. The "apparent" air-to-vacuum focus shift was between 0.013 and 0.0135 inch. The focus uncertainty could be drastically reduced if a simulator with photographic capability was available in which the thermal and vacuum environment of the mission could be duplicated.

2. Section 2.2. The optimum focal position for the Petzval lenses of the 1100 series panoramic cameras is approximately 0.0005 inch further away from the field flattener than the

---

* Controlled Range Network.

† Ground resolved distance.

‡ High priority list.

focal position at which the low contrast (2:1) resolution of the lens reaches a peak. Experimentally, the optimum focal position of a lens can be determined by performing dynamic resolution versus focal position tests under various amounts of IMC mismatch between the panoramic camera and the target wheel. If these tests are performed in an ambient atmosphere (this is the present capability), an accurate correction must be made to the focal position for the air-to-vacuum focus shift.

3. Section 3.3. Seventy-five percent of the resolution predictions for the CORN targets correlate favorably with the actual readings.

4. Section 3.4.1. For the HPL targets, the average altitude of photography was 87.9 nm. Approximately 10 percent gain in scale could be achieved by reducing the average altitude of photography for these targets to 80 nm.

5. Section 3.4.2. The V/h programming errors seem to be within the allowable rms error of 1.5 percent. However, 22 percent of the frames checked had V/h errors larger than 1.5 percent, and it seems that it should be possible to reduce the V/h error to less than 1.5 percent for essentially all the frames of a mission.

6. Section 3.4.3. In this section, a study was carried out to determine possible ways of improving the resolution performance of the 1103 panoramic system with respect to the HPL targets. This study showed that a 19 percent improvement in resolution performance would have been achieved if the following conditions had prevailed:

a. Both lenses were focused to maximize tri-bar resolution.*
b. The average altitude of photography was 80 nm.
c. Type SO-230 or SO-205 film was used instead of Type 3404.

* Both lenses were initially focused in ambient to maximize the low contrast resolution. Then the focus error was introduced by an apparent air-to-vacuum focus shift of about 0.0133 inch instead of the anticipated value of 0.014 inch.

2. ANALYSIS OF FOCUS PROBLEM

2.1 AIR-TO-VACUUM FOCUS SHIFT

Compared with mission 1102, mission 1103 was a disappointment. As mentioned in the PET Report, the main degrading factors of the performance of mission 1103 were thought to be severe haze conditions extended over large geographical areas and improper focusing of the panoramic cameras. Before the mission took place, the cameras had been dynamically focused optimally on the basis of the information available at that time. An air-to-vacuum focus shift of 0.014 inch had been assumed, and tri-bar resolution versus focal position curves had been obtained by photographic tests. The position of the film in each camera had been adjusted to coincide with the focal position which produced the maximum low contrast resolution. Another implied assumption was that the focal position which produces the maximum low contrast resolution also results in the best aerial photography for a specific lens. This assumption is true for a truly diffraction-limited lens, but ought to be investigated for any other lens design.

The factors that could produce focusing errors are:

1. Air-to-vacuum focus shift other than 0.014 inch
2. Vacuum film lift above focal plane rollers different than air film lift
3. Lens focus shift due to mission thermal environment
4. Optimum focal position of lens for aerial photography different than focal position of peak resolution.

The contractor's computer program which is utilized for predicting lens performance and characteristics indicates that the air-to-vacuum focus shift is 0.0141 inch for all Petzval lenses of the 1100 series. Visual experiments on the air-to-vacuum focus shift showed that the shift is 0.0140 to 0.0145 inch. Other static photographic resolution experiments (with UTB film and W-25 filters) showed that the air-to-vacuum focus shift is somewhere between 0.0128 and 0.0138 inch and apparently varies between lenses of the same generation. These same experiments also showed that the vacuum focal position of maximum resolution can be determined significantly more accurately than the respective focal position in air. This observation is in agreement with other investigations which showed that the refractive index of air is affected by temperature, barometric pressure, relative humidity, and CO_2 content. Therefore, while the vacuum peak focal position is only a characteristic of the lens, the air peak focal position is, in addition, a function of all the variables which affect the refractive index of air. The barometric pressure has the most significant effect on the air peak focal position (or equivalently the air focal length) of the lens. The focal length of the lens increases by 0.00047 inch when the barometric pressure increases 1 inch of mercury. On the other hand, a 10 °F temperature rise decreases the air focal length by 0.00029 inch. In addition, an increase in relative humidity of 50 percent increases the air focal length by

0.00018 inch. Note that the temperature effect discussed here is related to the air focal length only through the change it produces on the refractive index of air. This temperature effect should be clearly distinguished from other temperature effects (discussed below) on the lens itself which influence the behavior of the lens whether in vacuum or immersed in air.

It should be obvious that the inaccuracies of determining the air peak focus can be considerably reduced by experimentally determining the air peak focus in a well controlled atmosphere. Even so, the technique of focusing the panoramic cameras in air is inherently inaccurate when compared with the dynamic focusing of cameras in vacuum, because even if the air peak focus could be determined (in a controlled atmosphere) as accurately as the vacuum peak focus, a correction to the focal position which is equal to the air-to-vacuum focus shift must be made. In turn, the air-to-vacuum focus shift is not known accurately, and, at best, can be determined by performing static photographic experiments on the lens utilizing a vacuum chamber with the added capability to produce a well controlled atmosphere. Even with this chamber, the error in determining the air-to-vacuum focus shift is expected to be approximately 1.4 times larger than the error in the vacuum peak focal position. Therefore, one reaches the conclusion that the only accurate method is to focus the lenses in vacuum. In that respect, the dynamic vacuum focusing of a complete camera in a vacuum chamber with photographic capability is the most desirable method. A somewhat less accurate but more practical technique is to focus each lens statically in a small vacuum chamber and later make a small adjustment for the dynamic film lift above the focal plane rollers.

There is, of course, another technique for focusing the cameras—the old, relatively simple trial and error method. Each system's focus is adjusted on the basis of the focus settings of the previous systems and their apparent mission focus conditions as well as they can be deduced from examination of the original negatives. This technique, of course, is a last resort and obviously is no substitute for an accurate and dependable laboratory focusing technique.

There are some indications that the vacuum film lift is somewhat different than the dynamic film lift in air. However, accurate and reliable data on this problem are not presently available.

On the basis of the information presently available, the lens focus shift due to the thermal environment of the mission appears to be less than 0.0003 inch. An investigation is being conducted at the present time to analyze the effects on the lens performance of the day-to-night thermal gradients resulting from the orbital motion of the vehicle.

Following the 1103 mission, a group of photographic resolution tests (known as the DRT* chamber tests) were performed on the 1109 panoramic system utilizing a large vacuum chamber which was made available on a temporary basis. The results of the tests are described in Appendix E. One sequence of these tests showed an air-to-vacuum focus shift of 0.0133 inch for the AFT-looking camera (having a second generation lens) and a corresponding shift of 0.0146 inch for the FWD-looking camera (having a third generation lens). Since the 1103 cameras both carried second generation lenses, it was suspected that perhaps the air-to-vacuum focus shift for the 1103 system was 0.0133 inch rather than 0.014 inch which was the originally expected air-to-vacuum focus shift. In addition, it was found that if an air-to-vacuum focus shift of 0.014 inch was assumed, the CORN target predictions did not correlate well with the actual readings (see Sections 3.1 through 3.3). However, if the air-to-vacuum focus shift was assumed to be 0.0133 inch, a favorable correlation could be established between the CORN target predictions and the actual readings.

*Dynamic resolution test (DRT).

Thus, it seems that the "apparent" air-to-vacuum focus shift for the 1103 system is 0.0133 inch. The term "apparent" includes not only the actual air-to-vacuum focus shift but also all the factors that affect the position of the film with respect to the lens peak focus.

2.2 OPTIMUM FOCUS FOR AERIAL PHOTOGRAPHY

The preceding section was centered about the problem of determining the mission peak focus position with respect to the film (essentially determining the position of the film on the dynamic resolution versus focus curve of the lens (see Figs. 3-1 through 3-4). Basically, this problem has been created by the inability to simulate the mission environment in the laboratory and to simultaneously perform photographic resolution tests. Now the attention of the reader is directed towards a different problem which has been successfully resolved. This problem is described below.

Suppose the position of the resolution versus focus curve can be accurately predicted before the mission takes place. Then one raises the question of how the film position should be adjusted with respect to the resolution versus focus curve in order to achieve optimum focus for the targets which are being photographed. If the targets of interest were tri-bar resolution targets, then obviously the film position should be adjusted to coincide with the expected position of the peak of the resolution versus focus curve. However, most real targets do not resemble tri-bar resolution targets.

Each specific target of interest has its own two-dimensional Fourier transform in which certain spatial frequencies will have larger amplitudes than others. If all possible targets are considered, it is to be expected that, on the average, all spatial frequencies will have approximately equal amounts of energy and therefore are of equal importance. In this case, for the average target, the best photography can be obtained by adjusting the focus of the lens so that the lens is the best possible approximation to the diffraction-limited lens of the same aperture and focal length. The diffraction-limited lens has no aberrations, and, when a plane wavefront of light enters the lens through the front element, it emerges through the last element as a purely spherical wavefront which converges on the point of optimum focus. On the other hand, a real lens has aberrations which produce distortions on the spherical wavefront. The root mean square (rms) deviation of the actual wavefront from the spherical wavefront is a measure of the quality of the lens. The rms wavefront distortion is expressed as a fraction of wavelength. The focal position at which the rms wavefront distortion reaches a minimum is the focal position at which the lens most closely approximates the diffraction-limited lens. Therefore, it was reasoned that for the average target, the best photography should be obtained by adjusting the film position so that it coincides with the focus position at which the rms wavefront distortion of the lens is minimum. Consequently, it became necessary to determine the relationship between the focal position which produced the maximum tri-bar resolution and the focal position which produces the minimum rms wavefront distortion. Thus, a theoretical investigation was conducted on a third generation lens with a W-25 filter and on a second generation lens with a W-21 filter. This investigation showed that for the third generation lens, the minimum rms wavefront distortion lies 0.0004 inch further away from the field flattener than the low contrast (2:1) resolution peak, while for the second generation lens, the corresponding displacement is 0.0005 inch. The results imply that the optimum focal position for general photography lies approximately 0.0005 inch beyond the low contrast resolution peak. The theoretical results have been confirmed by data collected on systems 1105 and 1109. (Explanations of these tests and interpretations of their results can be found in Appendices E and F.

In order to focus a camera for the minimum rms wavefront distortion, the usual resolution versus focus curve would be obtained and the film would be set at a position 0.0005 inch further away from the field flattener than the peak of the low contrast resolution versus focus curve.

However, since the determination of the peak of the resolution versus focus curve might be inaccurate, a more dependable technique requires performing dynamic resolution tests and varying the target wheel speed as well as the focus. At each focal position (increments of 0.0005 inch), a resolution versus image smear curve is obtained. The focal position which produces the maximum resolution curve for image smear larger than 2 to 3 microns lies within 0.00025 inch of the focal position which produces the minimum rms wavefront distortion. This technique had already been recommended in the 1101 performance report. In addition, the technique has been applied to the 1105 system, and the focusing recommendations for the 1105 system resulting from it coincide with the final focus settings of this system which were based on the performance of the 1104 system (assuming an air-to-vacuum focus shift of 0.0135 inch).

It has been known for a long time that tri-bar resolution data obtained at the contractor's laboratories display large fluctuations. These fluctuations are not due to equipment malfunctions but are a characteristic of and result from the statistical nature of the resolution data. Thus, individual resolution readings may be in error by a significant amount. In order to reduce the errors in the data, it has been customary, in the contractor's laboratories, to obtain at least five independent resolution readings under identical experimental conditions and average them, the result being a more accurate resolution number. Since the accuracy of the resolution data affects the accuracy with which a panoramic camera may be focused, it was decided to evaluate the accuracy of the resolution data and determine the most accurate technique of combining the resolution numbers. For this reason, a static photographic experiment was conducted utilizing a third generation lens and a W-25 filter. One hundred exposures were obtained on Type SO-380 film of a $^{6}\sqrt{2}$ high contrast target and a $^{12}\sqrt{2}$ low contrast target. Resolution readings were then obtained from the photographic images of the targets and their statistics were determined.

For the low contrast readings, the standard deviation of a single reading was computed to be approximately 20 lines per millimeter, while the mean was approximately 160 to 170 lines per millimeter. By averaging five readings, the standard deviation can be reduced to approximately 9 lines per millimeter. The average of 10 readings would have a standard deviation of approximately 6.5 lines per millimeter. However, the analysis of the statistics obtained from the experiment showed that if 10 independent resolution readings were available and five of them were averaged by eliminating the highest and four of the lowest readings, the resulting resolution number would have a standard deviation of approximately 3.5 lines per millimeter and would, of course, be larger than the average of the same 10 readings. Since most of the experimental conditions that cause the resolution reading fluctuations always reduce the resolution numbers, the higher average obtained by this new technique should be acceptable. In addition, for the purpose of focusing the panoramic cameras, whether the average resolution numbers are higher or lower is not important, but it is essential that the standard deviation of the averages obtained be as small as possible.

3. SYSTEM PERFORMANCE

3.1 CORN TARGET RESOLUTION

Each CORN target deployed consisted of the 51/51 tri-bar resolving power target, a Gray scale target, and a 100-foot edge target. These targets have already been described in the mission 1101 performance analysis report, so their description will not be repeated here. A more thorough explanation of these targets is also available in the CORN target manual.

Table 3-1 lists the geographic distribution of the CORN targets deployed. One was actually a fixed target (permanent installation). The first two columns labeled Pass and Frame uniquely identify the frame on which the image of a specific target display appears. The x and y coordinates listed in Table 3-1 pinpoint the position of the target image on the respective panoramic frame according to the universal grid system.

Table 3-1 — CORN Target Coverage

Pass	Frame	X, centimeters	Y, centermeters	Location
16	7 FWD	34	1	Edwards AFB, California, fixed
	13 AFT	42	2	target, 34°51′N, 117°45′W
16	14 FWD	45	1	Riverside, California, CORN target,
	21 AFT	30.5	1	33°50′N, 117°22′W
97	7 FWD	51	2	Napa, California, CORN target,
	13 AFT	24	4.5	38°22′N, 122°23′W
97	13 FWD	53	1	San Jose, California, CORN target,
	20 AFT	22	1	37°25′N, 122°11′W

The images of the CORN and the fixed target were examined by two observers who determined the corresponding ground resolved distances. The average readings are shown in Table 3-2. The readings were taken from the original negative. It is obvious that only a small number (four) of resolution targets were photographed in this mission. For the purpose of evaluating the system's performance, it would have been highly desirable to photograph more targets. It is understood that 13 CORN targets were deployed but only three were actually photographed.

For the targets of Table 3-2, the following information is pertinent if one tries to evaluate the system's performance utilizing the resolution readings:

1. FWD-looking camera, pass 16, frame 14. A W-12 filter was used to photograph this target instead of a W-25.
2. FWD-looking camera, pass 97, frame 7. The filter was being changed when this target was exposed.
3. FWD- looking camera, pass 97, frame 13. This target was also photographed with a W-12 filter.
4. AFT-looking camera, pass 16, frame 13. There is a possibility that this target might have been exposed while the slit was being changed.

Table 3-2 — Resolution Target Readings, Average of Two Readers

Pass	Frame	Along Track GRD, feet	Cross Track GRD, feet	Target Apparent Contrast
16	7 FWD	9	8	Medium contrast, fixed target
		7	8	High contrast, fixed target
	13 AFT	9	9	Medium contrast, fixed target
		6	8	High contrast, fixed target
16	14 FWD	16	12	1.60:1 (heavy haze) (W-12 filter)
	21 AFT	16	16	1.36:1 (heavy haze)
97	7 FWD	7.5	12	1.73:1 (filter being changed)
	13 AFT	10	8	1.89:1
97	13 FWD	7	12	1.75:1 (W-12 filter)
	20 AFT	7.5	12	2.05:1

Initially, the purpose of photographing a few CORN targets with the W-12 filter was to compare the performance of the FWD-looking camera using a W-12 and a W-25 filter. The W-12 filter allows shorter exposure times than the W-25, but produces lower contrast photography. Low contrast affects all spatial frequencies, while image smear resulting from long exposure times affects the high spatial frequencies only. When the image smear is an appreciable degrading factor of image quality (usually for exposure times longer than 3 milliseconds), an improvement in image quality can be achieved by selecting a Wratten filter which would reduce the exposure time to just under 3 milliseconds. It should be made clear, however, that this is only a rough rule of thumb, because, unfortunately, the selection of the optimum filter is influenced not only by the exposure times that will be required to expose a specific target, but also by the type of lens used (second or third generation) and atmospheric (haze) conditions over

the target. For example, if one wants to photograph a target shrouded by heavy haze, the best choice of filter for penetrating the haze would be a W-25 or even a W-29. However, a poor resolution performance should be anticipated because of the long exposure times associated with these filters. It should also be kept in mind that a filter like W-25 eliminates information present in a wavelength band which would have passed through a wider band filter. In other words, the narrow-band filters eliminate more information than the wide-band filters. In fact, for a target of peculiar color reflectances, a significant portion of the information associated with this target can perhaps be recovered by utilizing the SF-05 filter in one of the panoramic cameras and a W-21 or W-25 in the other camera.

As far as the W-12 versus W-25 filter test in the FWD-looking camera of system 1103 is concerned, the only information obtained is that the W-12 filter produces lower contrast photography than the W-25, a fact which was already known. It seems that this test had not been thoroughly evaluated before the mission took place, because the reduction in image smear achieved by the W-12 filter over the W-25 was not significant for the CORN targets of pass 97. Also, the CORN targets of pass 97 were apparently deployed close together and there was not enough time to change filters. On the other hand, this filter test eliminated the information that would have been obtained about the FWD-looking camera's performance with the W-25 filter. Since the CORN target readings are very important in evaluating and rating the panoramic systems, the CORN targets deployed in California or other areas which have consistently clear weather should be reserved for the primary filters. In addition, there is a need to perform special filter experiments. Obviously, the number of CORN targets deployed and photographed is inadequate.

3.2 DETERMINATION OF OPERATIONAL RESOLUTION

The method for determining the operational resolution is discussed more extensively in Section 3.2 of the 1101 performance analysis report.* This technique is described only briefly in the present section.

The dynamic camera resolution, image smear, and static lens-film resolution for any image point are related by the expression:

$$R_d = \frac{R_s}{[1 + (bR_s)^{E_1}]^{E_2}} \qquad (3.1)$$

where R_d = dynamic camera resolution
b = image smear
R_s = static lens-film resolution
E_1 and E_2 = experimentally determined exponents

Exponents E_1 and E_2 were determined from resolution versus image smear tests performed at the contractor's laboratory. Table 3-3 shows the exponents that were determined for the 1103 FWD- and AFT-looking cameras. The static resolution, R_s, at a specific point of the panoramic format is dependent on the performance of the Petzval lens at the corresponding field angle, the focus position occupied by the film, and the film characteristics. Thus, for all practical purposes,

[redacted]

R_S varies over the panoramic format of a camera but is not a function of time (does not vary between successive frames). In fact, a contour map of R_S could be constructed over the panoramic format.

Table 3-3 — Mission 1103 Exponents

Aft			Forward	
E_1	E_2	Contrast	E_1	E_2
2.30	0.47	High	1.90	0.53
2.30	0.47	Low (2:1)	2.30	0.42

In the resolution predictions, the values of R_S are determined individually for each target. To accomplish this, the static resolution of the lens as a function of field angle and focal position (from laboratory data) are utilized. For a specific target image, its y coordinate immediately gives the field angle the image occupies. In order to determine the focus position the same target image occupies, it is necessary to review the film flatness tests which provide the relative focal position of the target image with respect to the center of format. Finally, the operational focal position at the center of the format can be obtained from the final dynamic resolution versus focus tests performed at the contractor's laboratory. The results of these tests have been plotted in Figs. 3-1 through 3-4. The anticipated focal position at the center of format during the mission is also shown in these figures. Having determined the field angle and focal position of a specific target, the associated R_S values are readily obtained.

The computation of image smear is also described in detail in Section 3.2 of the mission 1101 performance analysis report. Since it is not possible to compute the image smear exactly, a systematic image smear component, b_s, and a random component, b_r, are separately computed for each target image. Then, the total image smear, b_t, is determined by the equation

$$b_t = b_r + |b_s| \tag{3.2}$$

Factor b_t is introduced into Equation (3.1) and utilized in the computation of the dynamic camera resolution, R_d. In turn, the ground resolved distance is related to R_d by a scale factor affected by vehicle altitude, camera focal length, and location on the panoramic format of the target image. The ground resolved distance which is computed in this fashion is a probabilistic quantity. Thus, the predicted ground resolved distance is not equal to the actual ground resolved distance. Instead, the predicted ground resolved distance implies that the probability that the actual ground resolved distance is smaller than the predicted value is between 64 and 84 percent. Therefore, the average predicted ground resolved distance is larger than the average actual ground resolved distance.

Resolution predictions were computed for the CORN targets of Table 3-1 and the HPL targets of Appendix A. For these targets, the SRV tape recorder summary was examined to determine if an abnormal number of jet firings took place, which would indicate possible vehicle disturbances and unusually high vehicle rates. For all of the targets mentioned above, the jet firing activity appeared normal.

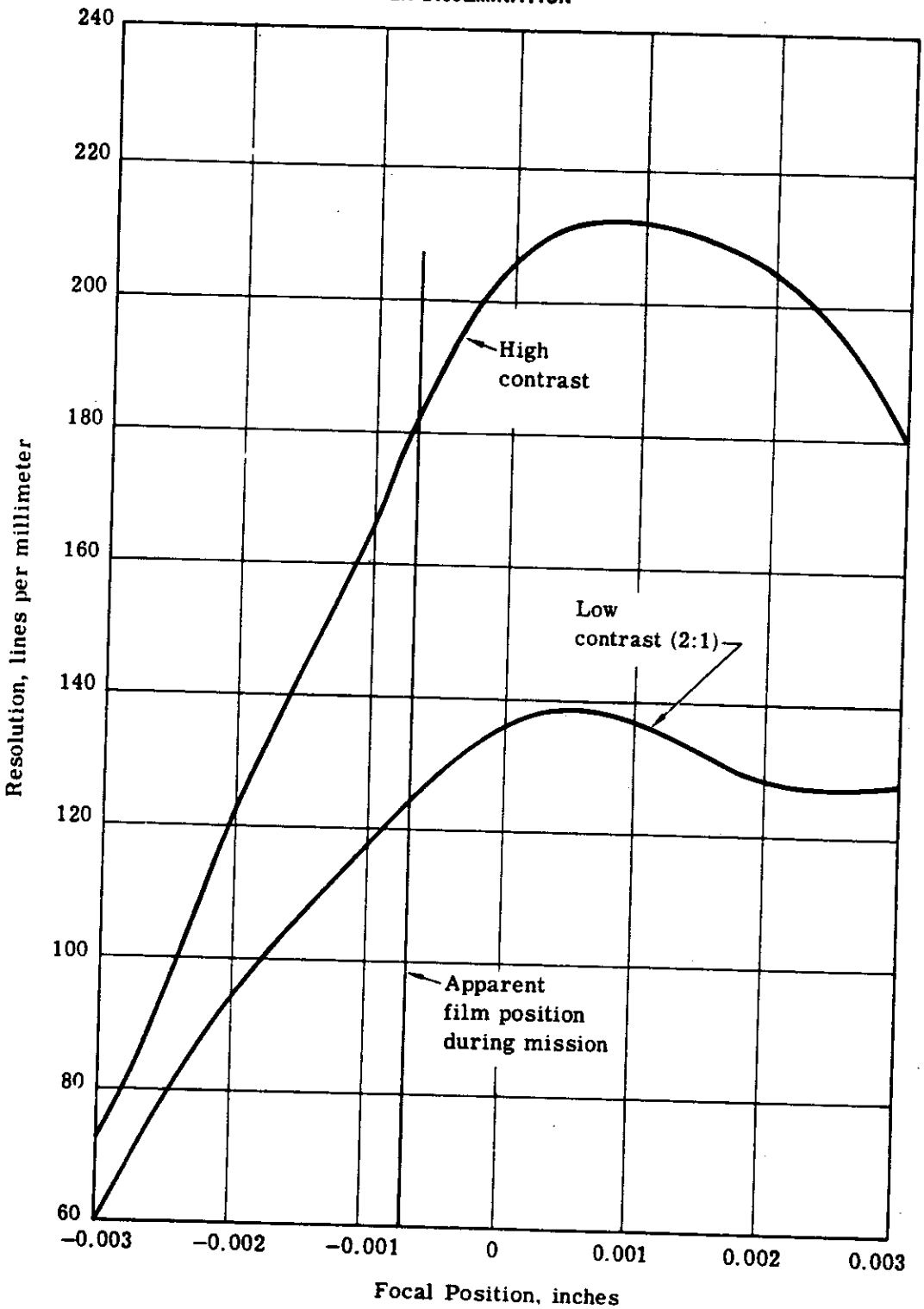

Fig. 3-1 — Dynamic resolution versus focus position, AFT-looking camera no. 306, along track

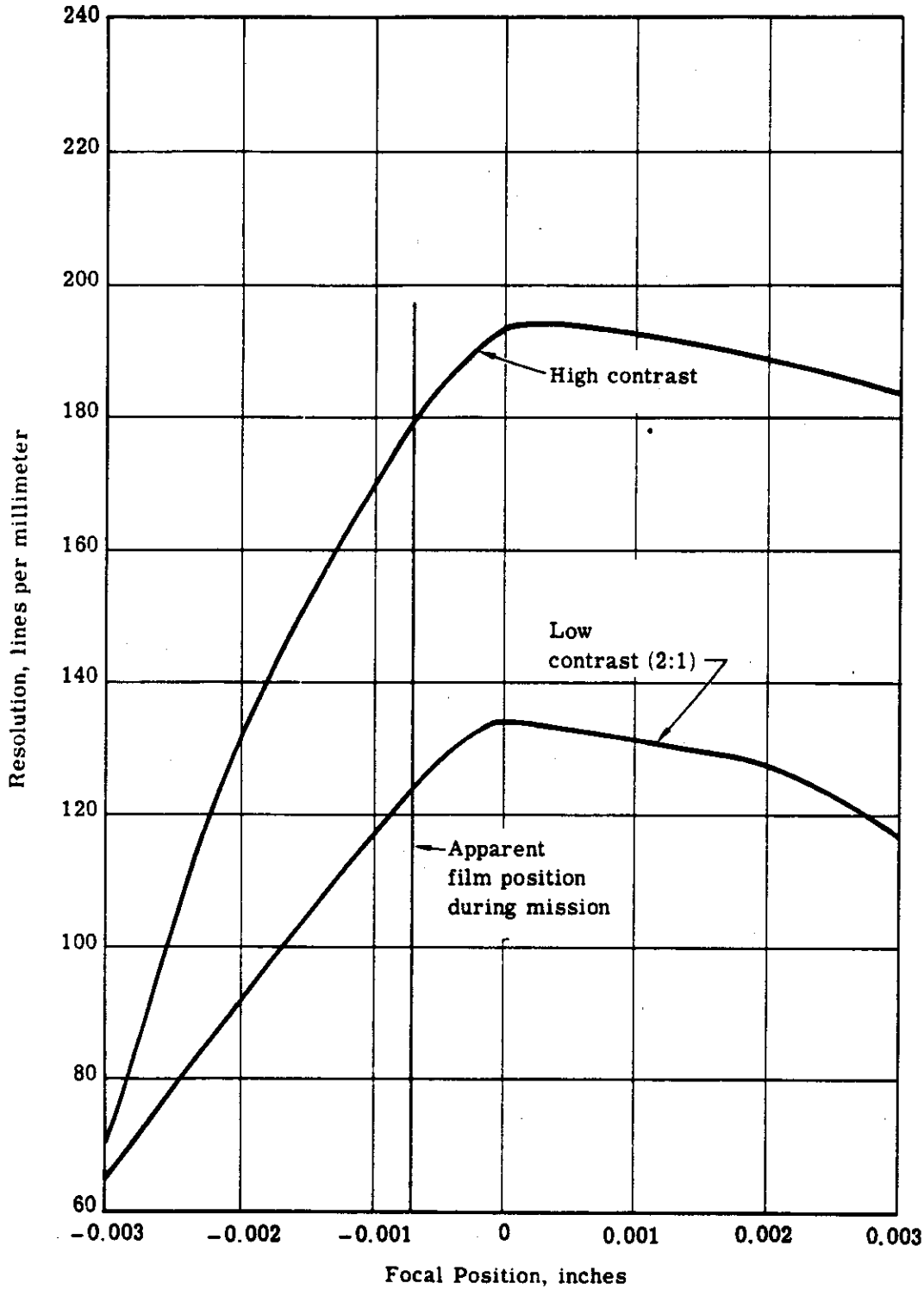

Fig. 3-2 — Dynamic resolution versus focus position, AFT-looking camera no. 306, cross track

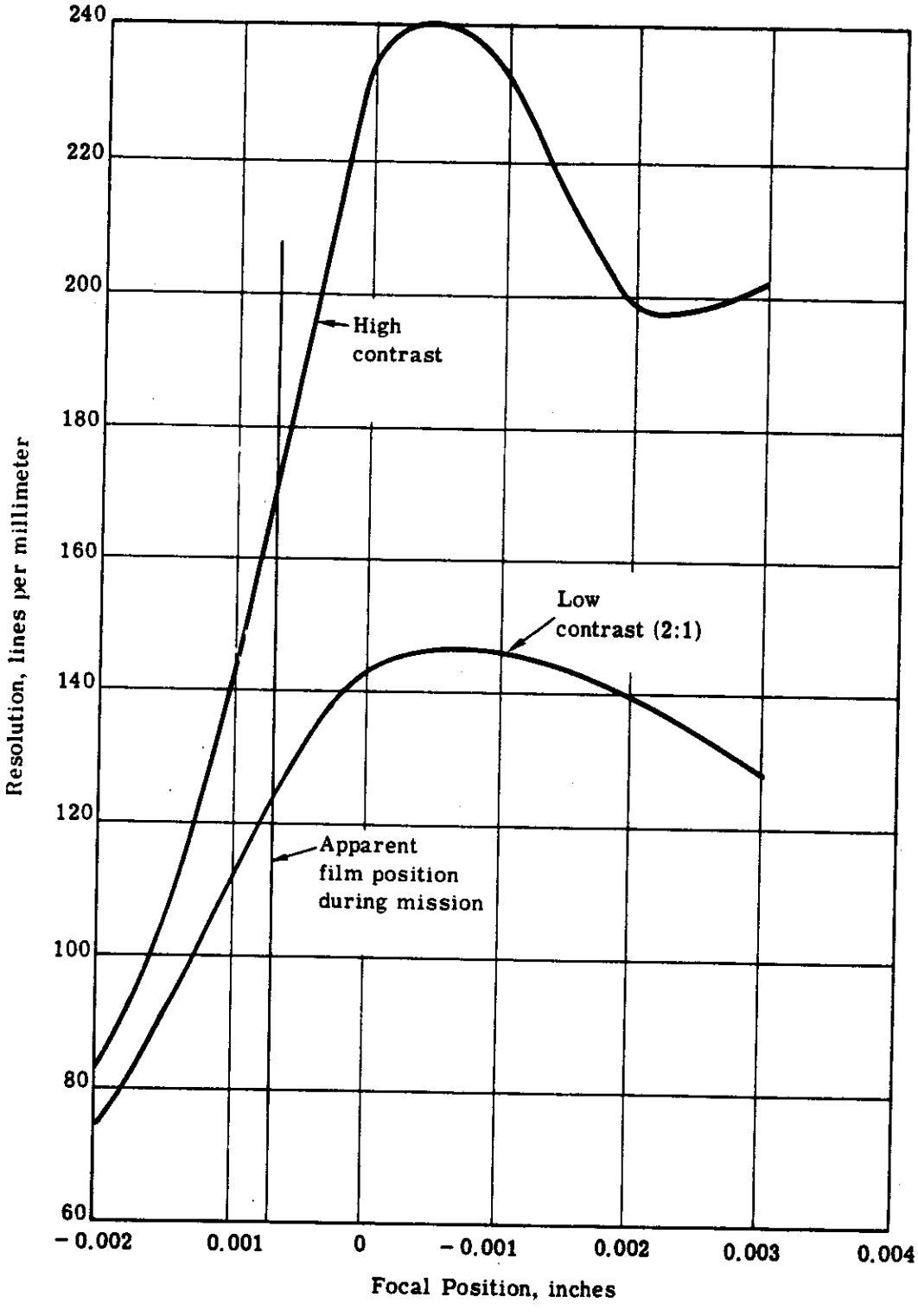

Fig. 3-3 — Dynamic resolution versus focus position, FWD-looking camera no. 307, along track

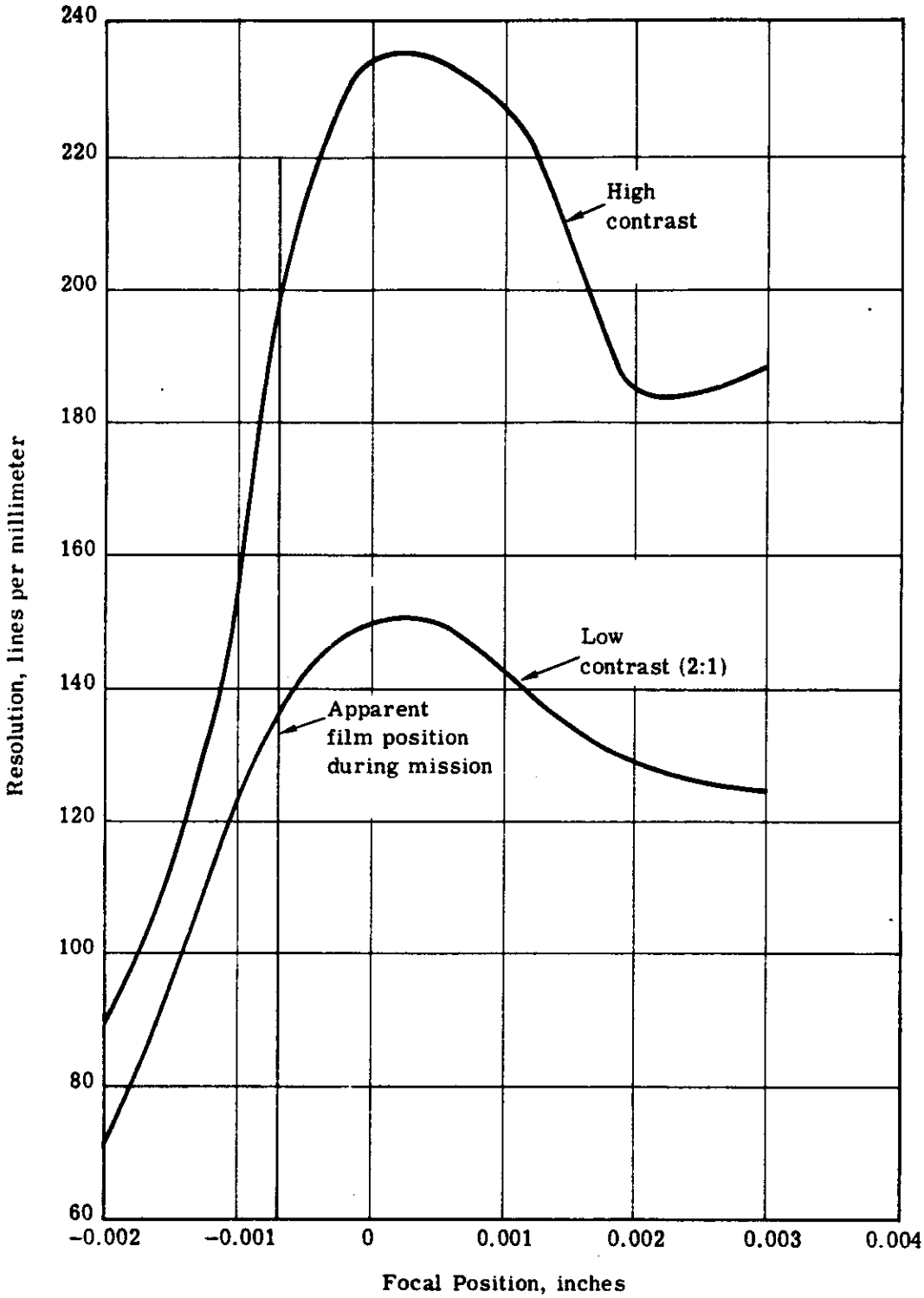

Fig. 3-4 — Dynamic resolution versus focus position, FWD-looking camera no. 307, cross track

3.3 COMPARISON OF CORN TARGET AND PREDICTED RESOLUTIONS

A fair comparison between a CORN target reading and the corresponding predicted ground resolved distance cannot be conducted without a knowledge of the apparent contrast of the target at the lens aperture. Resolution predictions have been computed for very high contrast and low contrast (2:1) tri-bar targets. On the ground, the contrast of the CORN targets is a nominal 4.7:1. The fixed targets are usually of higher contrast, approximately 10:1, but their real contrasts at the lens aperture are unknown, and depend on how well the targets are maintained.

On the other hand, during the photographic mission, the contrast of all ground objects including resolution targets is reduced by the atmosphere. The loss in contrast is affected by weather conditions as well as by solar elevation and azimuth. In Section 3.1 of the 1101 performance analysis report, the relationships between contrast and modulation are described. In the same section, a method for determining the apparent CORN target contrast at the lens aperture is also described. This method requires that microdensitometer traces be obtained on the original negative of the edge target which is part of the CORN target display. The fixed target displays have no edge targets. Thus, for the fixed targets, the apparent target contrast or modulation cannot be computed.

For mission 1103, the edge targets of the CORN target displays were traced with a microdensitometer by the Air Force Special Projects Production Facility. From these traces it was possible to compute the apparent tri-bar target contrasts shown in Tables 3-2 and 3-4.

Table 3-4 — CORN Target Readings and Predictions*

Pass	Frame	Along Track		Cross Track		Apparent Contrast
		Average Reading, feet	Predicted GRD, feet	Average Reading, feet	Predicted GRD, feet	
AFT-Looking Camera						
16	13	9	7.8	9	7.1	<2:1
16	21	12-16	7.7	12-16	7.7	1.36:1
97	13	10	6.9	8	7.5	1.89:1
97	20	7.5	7.1	8-12	7.9	2.05:1
FWD-Looking Camera						
16	7	9	8.6	8	6.9	1.73:1
97	7	7.5	7.0	8-12	7.2	1.73:1

* Predictions are for low contrast (2:1) targets.

Table 3-4 provides a means of comparing the CORN target readings with the predicted ground resolved distances. The column identified as Average Reading has entries which are the corresponding average readings taken from Table 3-2, except that some readings have been replaced by two numbers separated by a dashed line. This was deemed necessary because the CORN target display has only three panels for GRD's larger than 8 feet. These panels correspond to the following GRD's—8 feet, 12 feet, and 16 feet. Hence, whenever the reading is 12 feet, the actual GRD is somewhere between 8 and 12 feet. The predicted ground resolved distances are low contrast (2:1) values. No predictions were made for CORN targets photographed by the FWD-looking camera with the W-12 filter, because the required laboratory data for this filter do not exist.

Examination of Table 3-4 shows that 75 percent of the predicted ground resolved distances correlate well with the average target readings when the apparent contrasts of the targets are taken into account.

3.4 EVALUATION OF SYSTEM OPERATION

While the other sections of this report attempt to establish the performance level of the 1103 system, this section is devoted to methods and techniques which could have improved and optimized the 1103 system's performance. Hopefully, this kind of evaluation will provide valuable information for the optimization of subsequent systems.

3.4.1 Altitude of Photography

For the CORN and HPL targets for which resolution predictions were computed, the average altitude of photography turned out to be 87.9 nm. It should be obvious that the average ground resolved distance and the scale of the photography could be reduced almost 10 percent by photographing the HPL targets from an average altitude of 80 nm. Fig. 3-5 shows the altitude distribution of the HPL targets. Each point in this distribution represents one or more targets. Two targets photographed on revolutions no. 203 and 218 are not shown in Fig. 3-5. The HPL targets fall into the following categories according to their respective altitudes of photography:

1. Three targets between 95 and 100 nm
2. Six targets between 90 and 95 nm
3. Twenty targets between 85 and 90 nm
4. Seven targets between 82 and 85 nm.

Fig. 3-5 shows that the altitude of photography for the HPL targets is somewhat reduced as the mission progresses. The average geographic latitude for the HPL's is approximately 50 °N, with a standard deviation of approximately 7 degrees. However, for mission 1103, the perigee of the orbit was maintained throughout the mission at latitudes between 17 °N and 50 °N, and the altitude at perigee was not allowed to be reduced below 83.7 nm. Thus, it seems that the HPL targets for mission 1103 could have been photographed at an average altitude of 80 nm by maintaining the orbit perigee at approximately 50 °N and by reducing the perigee altitude to approximately 79.5 nm.

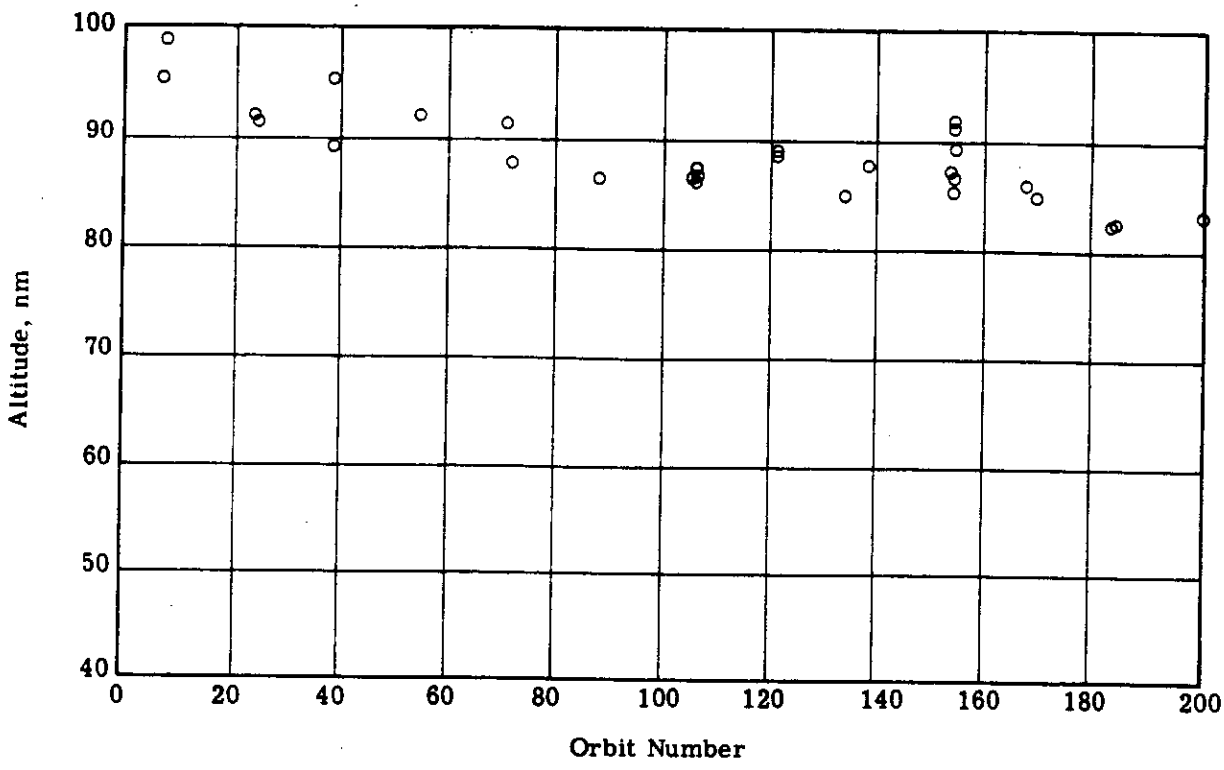

Fig. 3-5 — Altitude distribution of HPL targets

3.4.2. V/h Errors

The FMC rates of the panoramic cameras were checked against the required V/h rates computed from ephemeris data. This was done for 107 frames from both the FWD- and AFT-looking cameras. Of these, 72 frames contained the HPL targets. It was found that in pass 184, both cameras were running approximately 36.7 percent too slow, a gross error which was attributed to the V/h programmer. Since both cameras appeared to be running very closely at the same speed throughout the mission, it was considered that the major error between the FMC and V/h rates should be attributed to the V/h programmer. Excluding two targets from pass 184, the average percentage error for the remaining 105 frames turned out to be +0.11 percent, while the standard deviation from this mean was 1.31 percent. It appears that the performance of the V/h programmer has been improved and is within the requirement of 1.41 percent. However, 12 frames had a percentage error between 1.5 and 2.0 percent, 7 frames had a percentage error between 2.0 and 3.0 percent, and 3 frames had a percentage error between 3.0 and 4.6 percent. Thus, approximately 22 percent of the frames checked had an appreciable (larger than 1.5 percent) V/h error. On the other hand, 78 percent of the frames checked had a V/h error of less than 1.5 percent. Therefore, it appears that it should be possible to reduce the V/h error to less than 1.5 percent for essentially all the frames of a mission.

3.4.3 Ultimate Resolution Performance

Ways by which the performance of the 1103 panoramic cameras could have been optimized will now be considered. All possibilities that were considered fall under one of the following categories:

1. Reduction of image smear
2. Reduction of altitude of photography
3. Improvement of lens focusing techniques.

Various steps which would have improved the 1103 system performance with various degrees of success have been listed in Table 3-5. In Table 3-6, the average expected ground resolved distances for the cases described in Table 3-5 have been entered. In Table 3-6, an attempt has been made to use identical values for all parameters which should be invariant between any two cases. This is essential in order to make a valid comparison. At the same time, data from mission 1103 have been used in order to make the comparison directly applicable to this mission. The data utilized were obtained by averaging the respective data from the CORN and HPL targets. Thus, average image smear, average static lens resolutions, and average scale factors were determined for the CORN and HPL targets.

Case H shows the optimum performance level of which the 1103 system was capable. For this case, the following assumptions have been made:

1. Both lenses have been focused to maximize tri-bar resolution.
2. The average altitude of photography is 80 nm.
3. Type SO-230 or SO-205 film has replaced Type 3404.

A comparison of cases H and A in Table 3-6 shows that case H represents a 19 percent improvement in performance over case A, approximately 10 percent of which can be attributed to the reduction in the altitude of photography to 80 nm. More significantly, the operational requirements imposed by case H (the three assumptions discussed above) should be well within the realm of possibility.

Table 3-5 — List of System Configurations

Case	Description
A	Actual mission 1103 configuration
B	Identical to A except the average altitude of photography reduced to 80 nm
C	Identical to A except the cameras focused for maximum resolution
D	Identical to C except the average altitude of photography reduced to 80 nm
E	Identical to A except that Type 3404 film replaced by Type SO-205 or SO-230
F	Identical to E except that the average altitude of photogaphy reduced to 80 nm
G	Identical to C except that Type 3404 film replaced by Type SO-205 or SO-230
H	Identical to G except the average altitude of photogaphy reduced to 80 nm

Table 3-6 — Comparative Chart of Average System Performance, Low Contrast GRD

Case	FWD-Looking Camera		AFT-Looking Camera	
	Along Track GRD, feet	Cross Track GRD, feet	Along Track GRD, feet	Cross Track GRD, feet
A	8.0	8.1	7.6	8.5
B	7.3	7.4	6.9	7.8
C	7.5	7.7	7.4	8.4
D	6.8	7.0	6.8	7.6
E	7.7	7.3	7.4	7.8
F	7.0	6.7	6.8	7.1
G	7.1	6.8	7.3	7.6
H (Goal)	6.5	6.2	6.6	6.9

4. A-TAKEUP EXPERIMENT

4.1 GENERAL

The purpose of this experiment was to measure three image quality parameters as a means of detecting changes in the original negative imaging characteristics accrued during mission environment. Measurements of (1) resolution as a function of contrast, (2) granularity as a function of density, and (3) modulation transfer as a function of spatial frequency were made on both mission-recovered Type 3404 samples and two different Type 3404 control samples.

The payload sample (identified as "A-takeup") was an initial length of film (3404-401) removed from the A-takeup cassette of the 1103-1 recovered capsule. Proximate control (identified as "Preflight") was a sample of 3404-401 taken from the odd serial number 1103 supply cassette just before installation into the capsule. Ultimate control (identified as "Control") was a sample of film (3404-406) taken from the film contractor's refrigerator master supply.

A possible weakness of this experiment is the fact that this "A-takeup" film was run through the camera on the pad before lift-off under ambient ground conditions. Because the film is somewhat protected on the core by subsequent film convolutions, it is questionable whether this film has experienced the full impact of the 1103 mission environment. However, it is the best method available for this type of study, being one step more refined than an analysis of material having no environmental history at all.

Replicate exposures of tri-bar resolution targets (at selective contrasts), uniform patches (at selective luminance levels), and straight edges (at a single contrast) were made by the processing contractor on each of the three experimental samples. These exposures were all made at one given time in a microscope objective camera arrangement with a simulated daylight source modified by a W-23A filter. The samples were then processed along with the mission film. Measurements and analyses were carried out by this contractor. Fig. 4-1 displays the structure of the experiment in summary form.

Results indicate that the Type 3404 film flown in the 1103-1 mission underwent no appreciable change in imaging characteristics. Comparison with the similar experiments performed on the 1102 and 1101 missions reveals some inconsistencies in the data which will require at least one other similar experiment to resolve.

4.2 RESOLUTION AS A FUNCTION OF CONTRAST

Standard $^{6}\sqrt{2}$ tri-bar resolution targets of six different contrasts were imaged onto the three Type 3404 film samples in sets of three replications at each of 11 exposure levels. Each recorded target was read individually by three different readers. The consequent sets of nine values for the condition of best exposure were statistically analyzed for mean and 95 percent confidence limits, and the results are shown in Table 4-1. All calculations were executed in logarithmic

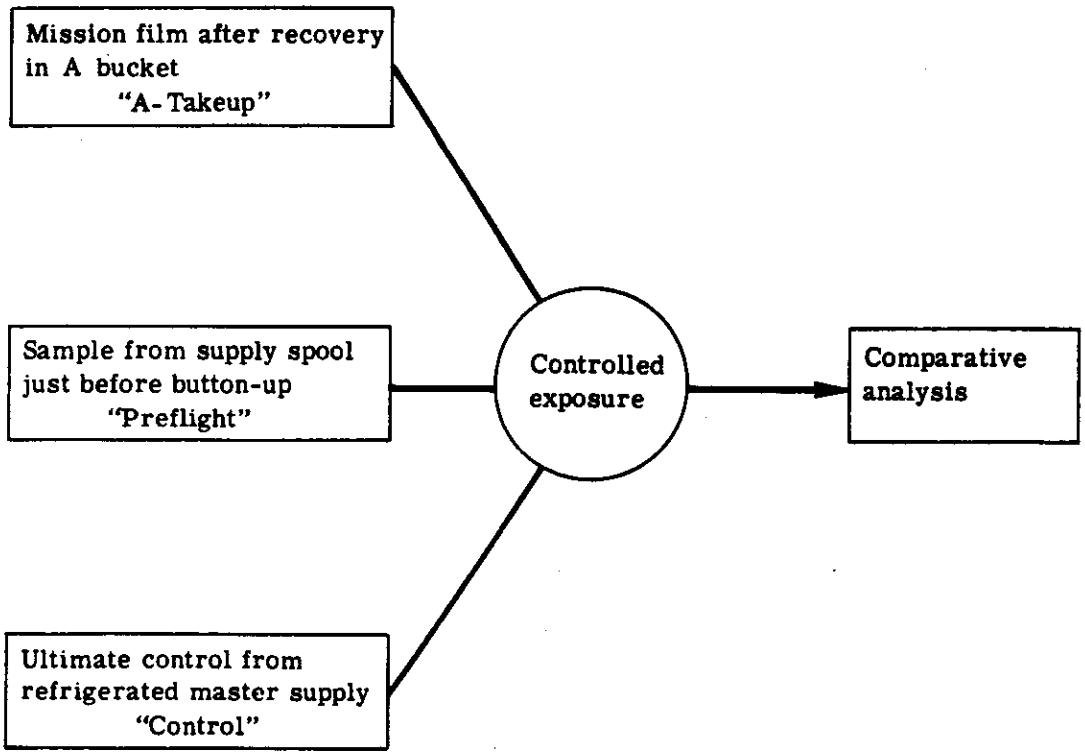

Fig. 4-1 — Structure of the A-takeup experiment

terms in order to properly weight the resolution target element progressions (in lines per millimeter) as a geometric function.

The data so reduced are presented graphically in Fig. 4-2 (a to c). Mean and 95 percent confidence limits are plotted for each of the three film conditions. For each set of data, an average curve is fitted to show the functional dependency of recorded target resolution on object target modulation. All of these curves are contained within the confidence limits associated with each of the three film conditions. Since the difference between the derived averages for these curves lies within the spread defined by experimental error, it is indicative that the 1103 A-takeup film underwent no appreciable change in imaging characteristics due to the mission environment. For ease in comparison, the curves for the test condition and the two control conditions are replotted together in Fig. 4-2(d).

Comparison of this 1103 data with that generated for the preceding two J-3 missions is shown in Fig. 4-3. Analysis of raw data bears out what these curves illustrate. There is an appreciable difference in resolution as a function of contrast for each of the three A-takeup experiments. For the most part, the 1101 curve oscillates between the 1102 and 1103 curves. At the same time, the clear-cut distinction between 1102 and 1103 is evident. It is interesting to note, however, that both of these sets of curves display a tendency to level off at a threshold value of 0.035 modulation.

Table 4-1 — Results of 1103 Resolution Data Reduction

Filter	Identification	Target Contrast	Target Modulation	Average Resolution, lines per millimeter	95 Percent Confidence Limits	
					Low	High
78 + 23A	Control (3404-406)	1.08:1	0.0384	33	26	41
78 + 23A	Control (3404-406)	1.15:1	0.0698	121	106	138
78 + 23A	Control (3404-406)	1.26:1	0.1150	164	149	181
78 + 23A	Control (3404-406)	1.70:1	0.2592	261	235	289
78 + 23A	Control (3404-406)	2.63:1	0.4490	378	378	420
78 + 23A	Control (3404-406)	5.14:1	0.6743	435	404	468
78 + 23A	Preflight (3404-401)	1.08:1	0.0384	37	33	42
78 + 23A	Preflight (3404-401)	1.15:1	0.0698	106	92	122
78 + 23A	Preflight (3404-401)	1.26:1	0.1150	147	130	165
78 + 23A	Preflight (3404-401)	1.70:1	0.2592	218	195	244
78 + 23A	Preflight (3404-401)	2.63:1	0.4490	368	336	403
78 + 23A	Preflight (3404-401)	5.14:1	0.6743	429	380	485
78 + 23A	A-takeup (3404-401)	1.08:1	0.0384	41	35	48
78 + 23A	A-takeup (3404-401)	1.15:1	0.0698	111	106	115
78 + 23A	A-takeup (3404-401)	1.26:1	0.1150	145	131	160
78 + 23A	A-takeup (3404-401)	1.70:1	0.2592	241	225	259
78 + 23A	A-takeup (3404-401)	2.63:1	0.4490	363	345	383
78 + 23A	A-takeup (3404-401)	5.14:1	0.6743	403	370	438

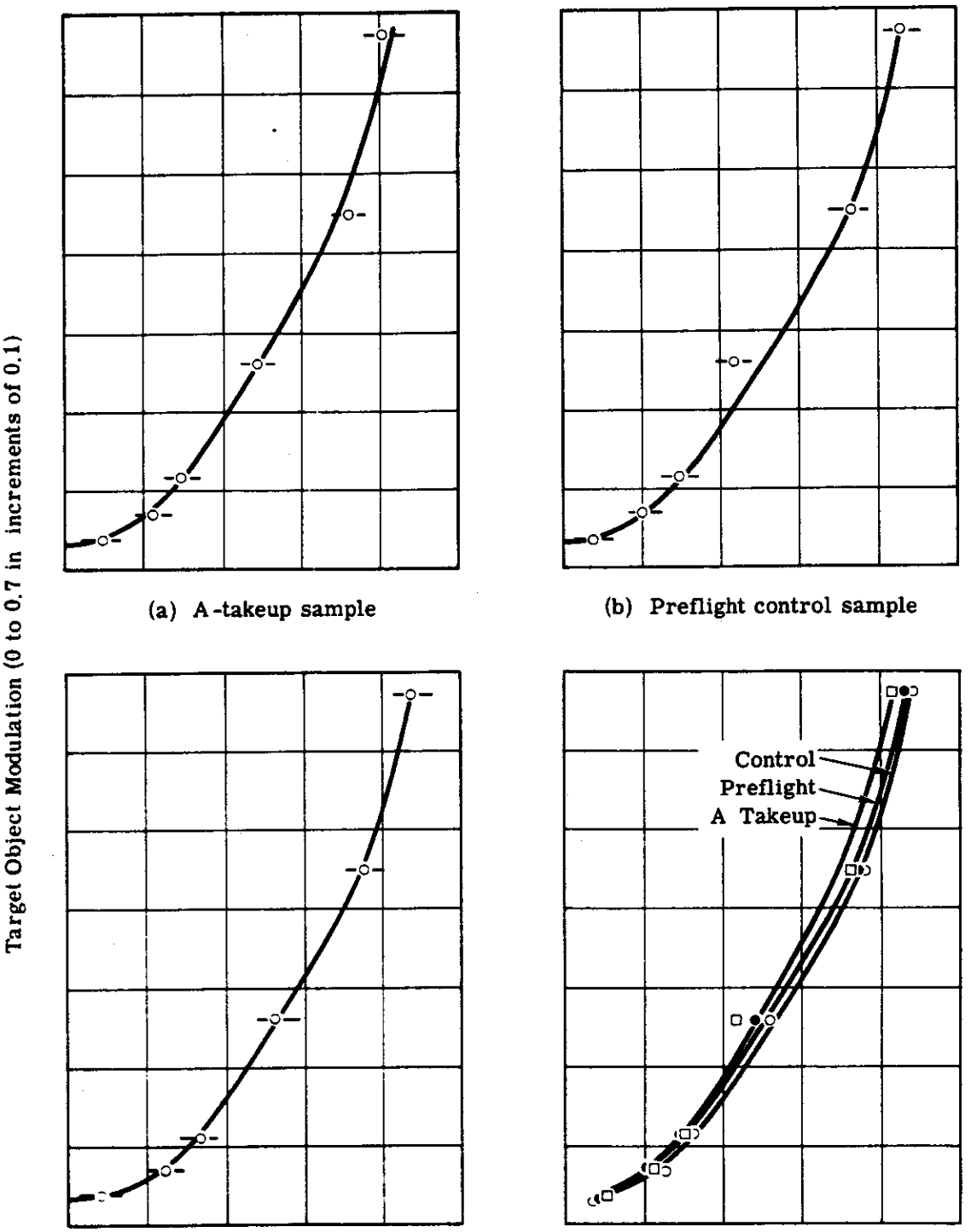

Fig. 4-2 — Target object modulation versus recorded target resolution for mission 1103 (horizontal bars represent real data contained within 95-percent confidence limits)

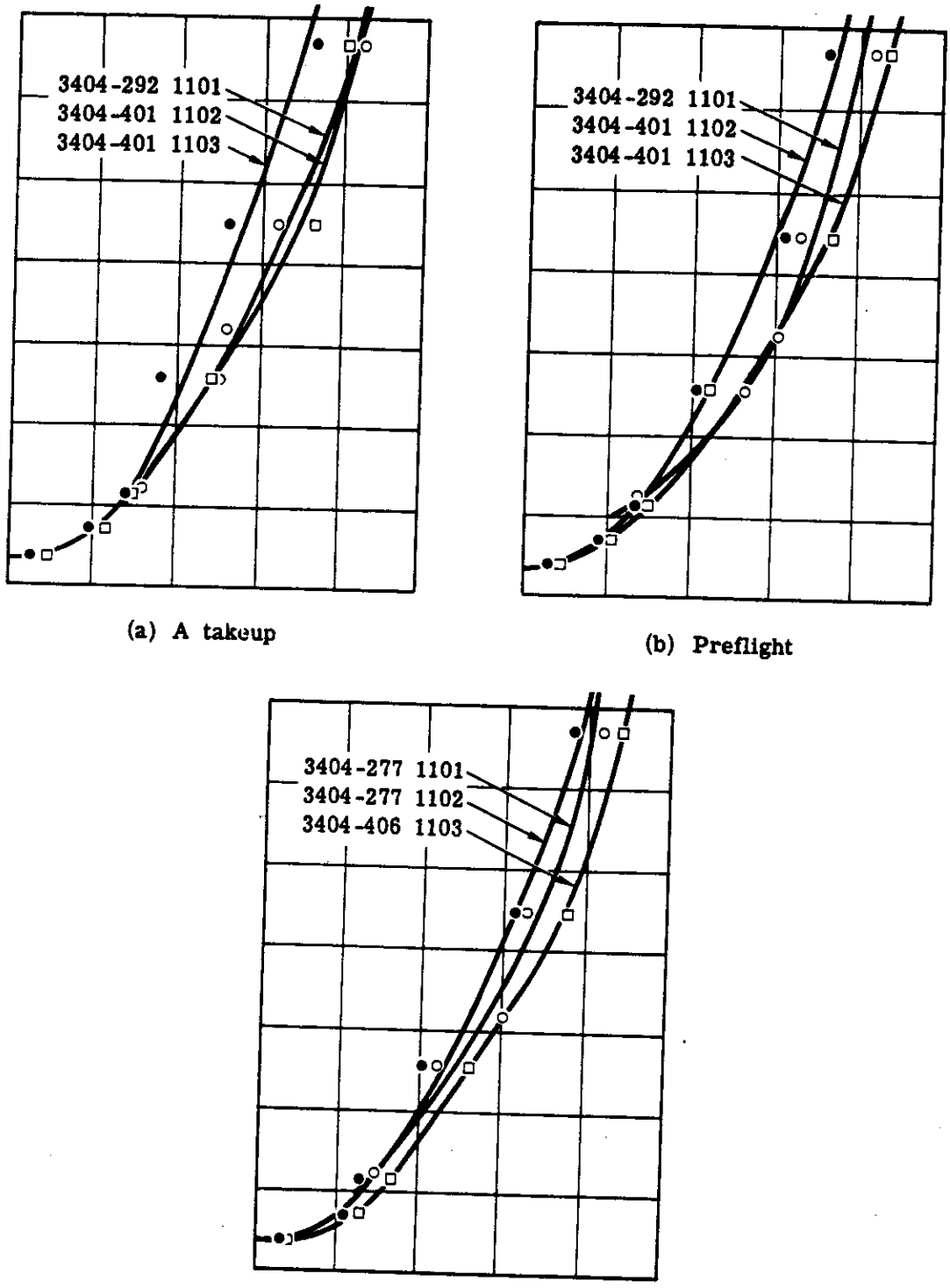

(a) A takeup

(b) Preflight

(c) Control

Resolution, lines per millimeter (0 to 500 in increments of 100)

Fig. 4-3 — Resolution as a function of contrast for each of the three film conditions on each of the three J-3 mission A-takeup experiments

4.3 GRANULARITY AS A FUNCTION OF DENSITY

Values of rms granularity were determined at four density levels for each of the three film conditions. The resultant data are plotted in Fig. 4-4, representing granularity as a function of density. Interpolated values of rms granularity at 1.0 gross density level are listed in Table 4-2 to comply with a comparison standard. The fact that these comparison values are nearly identical (0.031—0.033) suggests that there has been no alteration in the imaging characteristics of the 3404 emulsion due to the orbital environment. At the same time, the spread in the limited number of experimental data points producing anomalies in the projected curve shapes for the different missions indicates that the number of density levels sampled is insufficient to characterize the functional relationship between granularity and density in a smooth way.

The aperture size, 12 microns, was used because it was considered to be more in keeping with the viewing magnification to be used on the system product. To convert reported rms values thus determined to figures comparable to those obtained with a 24-micron aperture size, divide the values by 2 in conformance with Selwyn's Law.*

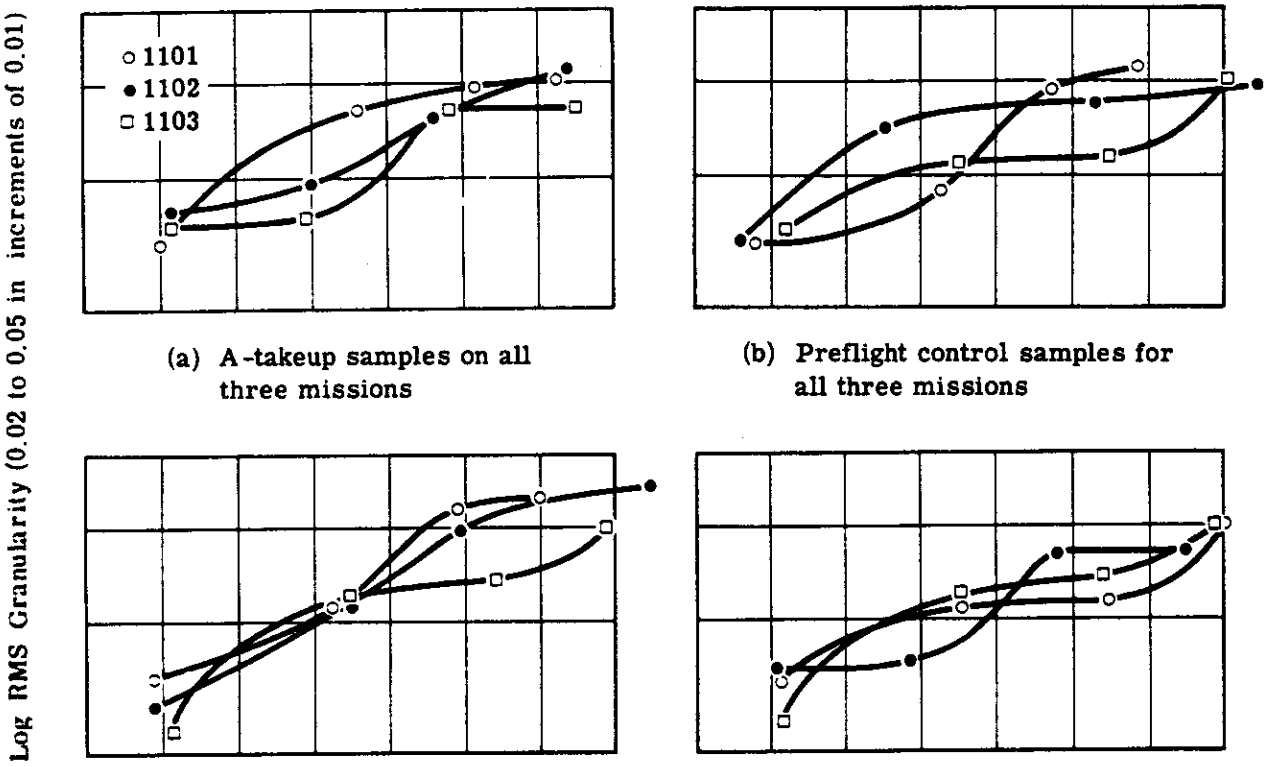

Fig. 4-4 — Granularity as a function of density

* Selwyn's Law states that granularity varies inversely proportional to the square root of the scanning aperture.

Table 4-2 — RMS Granularity at 1.0 Gross Density

Condition	1101	1102	1103
Control	0.036	0.035	0.033
Preflight	0.034	0.037	0.031
A-takeup	0.038	0.033	0.032

Aperture size	12 ± 1 micron
Data point spacing	Approximately 10-percent diameter overlap
Number of density patches per strip	4
Number of scans per density patch	5
Number of data points per scan	500

The rms granularity values were computed for each of 60 scans using bad data elimination and detrending techniques. A pooled estimate of the variance and rms value was calculated for each patch.

The granularity versus density curves in Fig. 4-4 for all three missions portray a general increase in rms value with increasing density. There is no tendency in these data for one mission experiment to be consistently different from the rest. The random intermixture of data points from each mission suggests that the variations are due to experimental error rather than any systematic symptom. Comparison between film conditions and between missions is made on the basis of rms granularity at 1.0 gross density as standard practice. Comparison between missions shows that the 1103 data indicates slightly lower granularity than the 1102 and 1101 data. Comparison between mission 1103 film conditions reveals that there has been no change in granularity in the payload film from the two control films.

4.4 MODULATION TRANSFER AS A FUNCTION OF SPATIAL FREQUENCY

4.4.1 Results

Modulation transfer functions for each of the two Type 3404 film control conditions and the one mission condition were computed from microdensitometric traces of low contrast edges exposed onto all of the film samples after completion of the 1103-1 mission. Comparisons have been made with the MTF's derived from the 1102-1 and 1101-1 A-takeup experiments. Results indicate that:

1. There is no significant difference in the A-takeup MTF from the two control MTF's.
2. The data variation in replicate determinations is about the same degree for the A-takeup as well as the two control MTF's.
3. All of the 1103 MTF's are about the same as the 1102 MTF's.
4. All of the 1101 MTF's are significantly higher than both the 1102 and 1103 MTF's.

4.4.2 Detailed Analysis

Each of the three film samples received a step tablet exposure and three replicate exposures to a low contrast edge in the Kodak Microscope Camera at one period of time and under the same

instrumental conditions. Lenses employed in the camera were a Zeiss 0.65 NA planapochromat 25× objective with a Zeiss Komplan 8× eyepiece for an overall reduction of −189×. The nine edges so produced exhibit nonsymmetrical properties and are generally characterized by approximately an 0.8 specular density difference. Edge spread varies in a 2:1 range, from 13 microns at best to 25 microns at worst, as shown in Fig. 4-5. Since there is no patterned relationship between edge spread and film condition, we know that there is no weighting of edge acuity to any particular test sample.

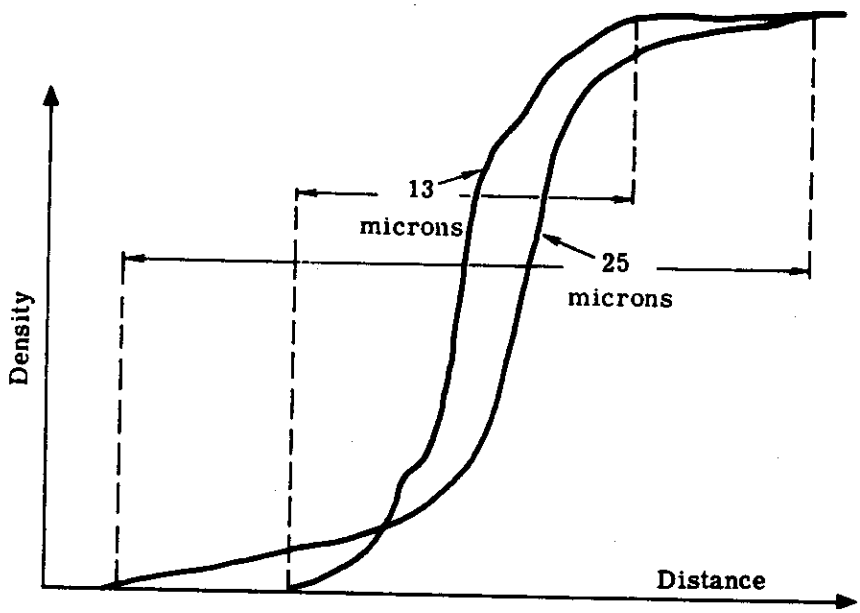

Fig. 4-5 — Comparison of the sharpest and broadest smoothed edges (All of the nine edges constituting the base data for this MTF analysis are contained within these limits.)

Each of the nine edges was traced on an Intectron microdensitometer with a 30- × 0.6-micron slit at five contiguous positions. Stepped densities from the calibrated wedge were also recorded. For each edge, the five microdensitometric traces were superimposed, matched with regard to density scale, shifted on the distance scale to achieve alignment of the linear portion of the traces, and then hand-smoothed onto an overlay. These averaged edge traces were then sampled at 0.25-micron increments to produce a 100-point data base for each curve. The step tablet exposure density values were data processed to produce the appropriate relative exposure base, and this information was loaded into the MTF computer program together with the edge data.

The computer MTF plots of Fourier calculated MTF's become noisy and, therefore, unreliable at very high frequencies, so the analysis is restricted to the 0-to-200-cycle-per-millimeter frequency domain. Experimental variation in the data is reflected in minor fluctuations and cross-over points. Envelopes were drawn to encompass these experimental fluctuations and a mean curve was drawn between them.

The mean curve, together with smoothed envelopes for each of the three test conditions, are reproduced in Fig. 4-6. Two points are evident: (1) the displacements in the means are contained within the degree of experimental variation, and (2) the three replicate MTF determinations have about the same degree of variation for all three test conditions.

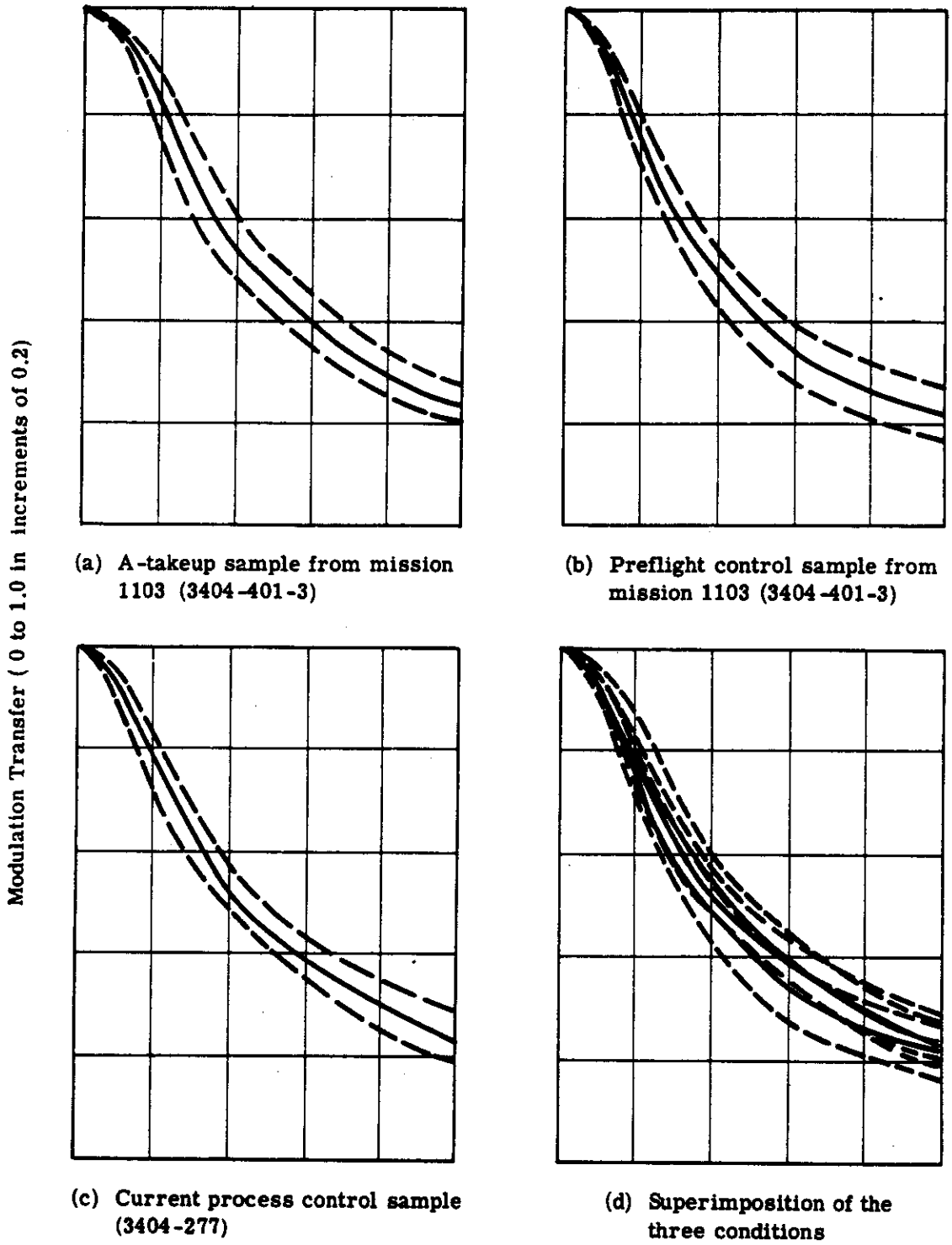

Fig. 4-6 — Average MTF's (solid lines) for each of the three test conditions with respective experimental variation (dashed lines)

Average MTF's determined from each of the first three J-3 mission A-takeup experiments are plotted for comparison in Fig. 4-7. The modulation transfer characteristics of film Type 3404 for each of the two control conditions and the payload condition as determined for missions 1103 and 1102 are similar. The same data derived from mission 1101 produced significantly higher modulation transfer for the entire frequency spectrum analyzed. Fig. 4-7(d) replots all of the average MTF's as well as the manufacturer's published MTF for Type 3404 film (EK dashed line) for ease of comparison. Because of the processing anomaly associated with the 1102 A-takeup experiment (see the [redacted] page 4-1), it was expected that the 1103 data would have been commensurate with the 1101 curves rather than the 1102 MTF's. The fact that just the reverse turned out to be the case indicates the need for further experimentation.

4.4.3 Recommendation

Within the context of each A-takeup experiment in the first three J-3 missions, no important differences in 3404 imaging characteristics have been detected, so that the essential objective of each test has been accomplished. From a summary point of view, however, it is undesirable to leave the 1101 discontinuity from 1102 and 1103 unexplained.

It was originally planned to perform a summary study after the completion of the 1104 A-takeup experiment. However, the 1104 A-takeup film sample was fogged beyond use, negating the experiment. Therefore, in order to produce a fourth set of data for a valid summary study, it is recommended that the A-takeup experiment be carried out on mission 1105. This should provide sufficient information for an accurate appraisal of processing conditions and analysis techniques, which are variables in the determination of film modulation transfer as a function of spatial frequency.

4.5 COMPARING THE THREE IMAGE QUALITY PARAMETERS

Granularity is a measure of the structure of developed image in terms of its conglomeration of silver grains or pervading photographic noise. Resolution is a measure of the developed image's ability to record fine detail in discrete statistical steps. Modulation transfer is a measure of the effect of light scattering in the emulsion during exposure due to the granular structure of the silver halide distribution. All three of these measures are concerned in different ways with the imaging characteristics of the prime recording material for the panoramic cameras.

There is no attempt in these analyses to quantify the information content of the mission material. The objective is rather to monitor the imaging characteristics of the film, independent of other image quality influencing elements in the camera. In each of the three image quality parameters measured there is substantial agreement between the values measured on the A-takeup film sample subjected to the mission environment and those measured on the two control film samples, Preflight and Control. From the data correlation in each of these three points of view, it is concluded that the original negatives for mission 1103 have recorded the ground information covered by the flight plan without any significant change in the photographic mechanism from what it would have done under ambient conditions.

Data correlation between the first three J-3 missions is not at all as high as it is between film sample conditions in any one of these missions. Yet there is no tendency for the data in any one mission to be consistently superior or inferior in all three image quality parameters. Although there is some indication that the 3404 emulsion for mission 1103 exhibited both higher resolution and lower granularity, this indication is denied by the MTF measurements. In such a situation, it must be concluded that any differences in the imaging characteristics of the 3404 emulsion flow in the first three J-3 missions are obscured by the experimental variations in measuring the three objective parameters.

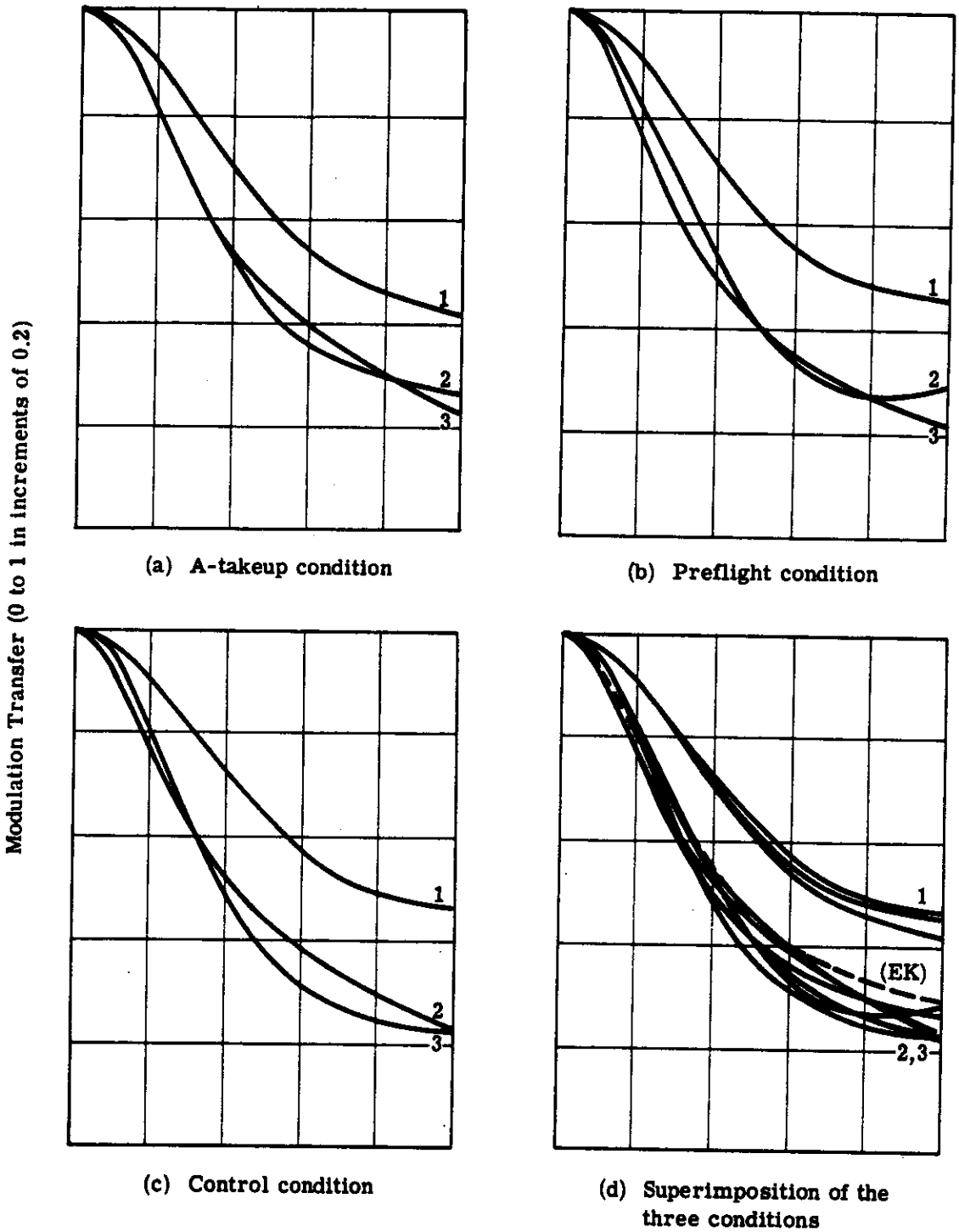

Fig. 4-7 — Average MTF's for 1101, 1102, and 1103 missions

5. DENSITY ANALYSIS

5.1 OBJECTIVE

Because of the complexity of uses for the payload photography, evaluation of the J-3 camera system with regard to proper exposure is a controversial issue. From the exchanges arising out of this issue has evolved a criterion for judgment that is meaningful for performance analysis.* This criterion centers attention on specific targets of strategic importance at a detail size commensurate with the image quality of the photography. It is tailored to take advantage of optimum tone reproduction at the lowlight and highlight extremes of the recorded targets, as revealed through microdensitometric analysis. A target whose exposure enters into the toe of its D-log E curve reduces discriminability of low-density differences. A target whose exposure enters into the shoulder of its D-log E curve reduces discriminability of high-density differences.

In these terms, the objective of this density analysis is to determine whether specific high priority targets on mission 1103 were properly or improperly exposed. These target density measurements are compared to the processing contractor's terrain density measurements in a continuing effort to establish the degree of correlation between the two techniques. Target density measurements were examined to reveal characteristic contrast relationships with regard to the filters flown in the 1103 mission.

5.2 PROCEDURE

Across each of 72 original negative target images, a single microdensitometric scan was made to characterize the target.† Location of the characterizing path was effected by subjective judgment to avoid any obvious misrepresentation of the target area. The scanning aperture was 10 microns in diameter, representing 8 to 10 feet on the ground. Calibration of the recorded densities was effected by periodic step tablet tracings. An image-representative value of minimum and maximum density was identified from each characterizing microdensitometer trace of an original-negative target.

Since both FWD and AFT coverage of each target were selected for tracing and because two target sites (112 and 302) were selected from two passes, a total of 34 different target sites were analyzed in mission 1103. Table 5-1 is a tabulation of the 72 minimum and maximum densities, measured along with corresponding data identifying pass, frame, camera, target number, slit, and filter. Note that 67 percent of the paired coverages analyzed were bi-color takes. This is compared to the 39 percent bi-color coverage for the mission as a whole.

---

* For a detailed examination, refer to KH-4B System Capability Report No. 2, [redacted]

† All measurements were made by NPIC.

Table 5-1 — Density Analysis of Mission 1103

Pass	Frame	Camera	Target	Slit	Filter	D_{min}	D_{max}	ΔD
D-007	013	F	120	0.205	W-25	0.80	1.12	0.32
D-007	020	A	120	0.160	SF-05	0.85	1.02	0.17
D-024	138	F	104	0.205	W-25	0.52	1.06	0.54
D-024	145	A	104	0.160	SF-05	0.86	1.15	0.29
D-025	008	F	229	0.205	W-25	0.56	0.80	0.24
D-025	014	A	229	0.135	W-21	0.52	0.82	0.30
D-039	117	F	31	0.205	W-25	0.93	1.10	0.17
D-039	123	A	31	0.160	SF-05	0.96	1.12	0.16
D-039	046	F	109	0.205	W-25	0.58	0.98	0.40
D-039	052	A	109	0.160	SF-05	0.63	0.88	0.25
D-005	008	F	117	0.205	W-25	0.66	0.81	0.15
D-005	014	A	117	0.135	W-21	0.73	0.92	0.19
D-071	005	F	116	0.205	W-25	0.54	0.98	0.44
D-071	011	A	116	0.160	SF-05	0.58	0.83	0.25
D-088	047	F	256	0.205	W-25	0.78	1.14	0.36
D-088	053	A	256	0.135	W-21	0.80	1.16	0.36
D-105	008	F	257	0.205	W-25	0.69	0.92	0.23
D-105	014	A	257	0.135	W-21	0.86	1.08	0.22
D-106	006	F	118	0.205	W-25	0.58	0.94	0.36
D-106	013	A	118	0.160	SF-05	0.70	0.96	0.26
D-106	025	F	223	0.205	W-25	0.52	1.04	0.52
D-106	031	A	223	0.160	SF-05	0.58	0.88	0.30
D-106	034	F	225	0.205	W-25	0.46	0.93	0.47
D-106	040	A	225	0.160	SF-05	0.62	0.88	0.26
D-106	036	F	252	0.205	W-25	0.48	0.86	0.38
D-106	042	A	252	0.160	SF-05	0.59	0.78	0.19
D-121	134	F	121	0.205	W-25	0.60	1.02	0.42
D-121	140	A	121	0.160	SF-05	0.64	0.90	0.26
D-121	118	F	123	0.205	W-25	0.68	0.88	0.20
D-121	124	A	123	0.160	SF-05	0.75	0.87	0.12

Table 5-1 — Density Analysis of Mission 1103 (Cont.)

Pass	Frame	Camera	Target	Slit	Filter	D_{min}	D_{max}	ΔD
D-134	011	F	714	0.205	W-25	0.66	1.08	0.42
D-134	017	A	714	0.135	W-21	0.66	1.02	0.36
D-138	045	F	113	0.205	W-25	0.52	0.80	0.28
D-138	051	A	113	0.135	W-21	0.66	0.92	0.26
D-138	048	F	801	0.205	W-25	0.42	1.10	0.68
D-138	054	A	801	0.135	W-21	0.46	1.10	0.64
D-153	028	F	124	0.205	W-25	0.75	1.03	0.28
D-153	034	A	124	0.160	SF-05	0.68	0.98	0.30
D-154	004	F	16	0.310	W-25	0.52	1.44	0.92
D-154	010	A	16	0.160	SF-05	0.55	0.90	0.35
D-154	017	F	101	0.310	W-25	0.53	1.25	0.72
D-154	023	A	101	0.160	SF-05	0.62	0.96	0.34
D-154	038	F	108	0.310	W-25	0.58	1.04	0.46
D-154	044	A	108	0.160	SF-05	0.58	0.84	0.26
D-154	134	F	209	0.205	W-25	0.53	0.90	0.37
D-154	140	A	209	0.160	SF-05	0.60	0.80	0.20
D-154	092	F	301	0.205	W-25	0.55	1.10	0.55
D-154	098	A	301	0.160	SF-05	0.66	0.93	0.27
D-167	012	F	119	0.205	W-25	0.52	1.07	0.55
D-167	018	A	119	0.135	W-21	0.66	1.12	0.46
D-183	005	F	41	0.205	W-25	0.48	0.92	0.44
D-183	011	A	41	0.135	W-21	0.57	1.00	0.43
D-183	015	F	850	0.205	W-25	0.63	0.99	0.36
D-183	021	A	850	0.135	W-21	0.70	1.08	0.38
D-184	010	F	36	0.205	W-25	0.73	1.20	0.47
D-184	014	A	36	0.160	SF-05	0.70	1.01	0.31
D-200	005	F	511	0.205	W-25	0.76	0.85	0.11
D-200	011	A	511	0.160	SF-05	0.88	0.98	0.10
D-200	008	F	512	0.205	W-25	0.52	0.88	0.36
D-200	014	A	512	0.160	SF-05	0.78	1.00	0.22

Table 5-1 — Density Analysis of Mission 1103 (Cont.)

Pass	Frame	Camera	Target	Slit	Filter	D_{min}	D_{max}	ΔD
D-200	008	F	303	0.205	W-25	0.62	0.92	0.30
D-200	014	A	303	0.160	SF-05	0.80	1.06	0.26
D-203	021	F	802	0.310	W-25	0.47	1.16	0.69
D-203	027	A	802	0.160	SF-05	0.55	0.89	0.34
D-008	006	F	112	0.205	W-25	0.63	1.02	0.39
D-008	012	A	112	0.135	W-21	0.61	1.06	0.45
D-218	013	F	112	0.310	W-25	0.46	0.90	0.44
D-218	019	A	112	0.160	SF-05	0.58	0.75	0.17
D-072	008	F	302	0.205	W-25	0.80	1.15	0.35
D-072	014	A	302	0.135	W-21	0.88	1.27	0.39
D-169	063	F	302	0.205	W-25	0.78	1.12	0.34
D-160	068	A	302	0.160	SF-05	0.84	1.04	0.20

This mission 1103 density analysis has the most extensive tracing data base to date. The mission 1102 density analysis covered 12 different target sites with 28 specimen tracings. The mission 1101 density analysis covered 14 different target sites with 32 specimen tracings. The mission 1043 density analysis covered 10 different target sites with 19 specimen tracings.

For Type 3404 film and its mission 1103 processing history, it has been decided that a minimum density below 0.40 is an underexposed condition, and a minimum density above 0.80 or a maximum density above 2.00 is an overexposed condition. These threshold values fulfill the requirements for the exposure criterion expressed above. These values are chosen to be meaningful for all three interrupted processing levels: primary, intermediate, and full. The value of 0.80 has been chosen as the D_{min} upper limit, since, with its particular curve shape for Type 3404, it would require a full stop less exposure to bring it down to the 0.40 level.

5.3 RESULTS

Examination of the maximum densities in Table 5-1 reveals that, of the 72 original negative images, none even come close to the 2.00 limiting value. The highest D_{max} recorded is 1.44 and the D_{max} values are concentrated in the 0.80 to 1.15 range. Since there is no threshold D_{max} value to identify underexposure, these readings indicate that the highlights of the high priority targets have been well recorded on mission 1103.

Looking at the minimum densities, there is no instance of D_{min} <0.40, which is interpreted to mean that none of the targets has been underexposed. On the other hand, there are 8 instances of D_{min} >0.80, and these indicate an overexposed condition for these particular targets on the 1103 mission. These eight exceptional targets were studied on first generation dupe positives, and some explanations of the overexposed indications became evident in terms of haze and cloud veiling.

	Rev	Frame	Camera	Target	Terrain/Atmosphere Conditions
1.	D-007	020	AFT	120	Loose blown snow or frost in the area; but not cause for overexposure
2.	D-024	145	AFT	104	Very clear atmosphere
3.	D-039	117	FWD	31	Target lies in cloud shadow and is seen through cloud veiling
4.	D-039	123	AFT	31	Almost totally obscured by veiling clouds
5.	D-105	014	AFT	257	Generally hazy atmosphere
6.	D-200	011	AFT	511	Localized haze
7.	D-072	014	AFT	302	Possible trail of veiling cloud over target
8.	D-169	068	AFT	302	Definite trail of veiling cloud over target

The terrain densities as determined by the processing contractor are shown in Table 5-2. The terrain measurements were made with a densitometer having a 0.5-millimeter spot aperture. The measured frames were chosen at random and the sample size was statistically determined so that a valid judgment could be made concerning the total mission. The mission was divided into four portions (the first and second buckets of the FWD and AFT cameras) and the total average minimum and maximum densities for each section are reported in their density/luminance profiles.*

Table 5-2 — [redacted] Terrain Densities

Mission	Camera	D_{min}	D_{max}
1103-1	FWD	0.62	1.37
1103-1	AFT	0.66	1.38
1103-2	FWD	0.48	1.34
1103-2	AFT	0.51	1.29

For comparison purposes, the target density analysis data of Table 5-1 were grouped into the same four portions and the D_{min} and D_{max} values were averaged. This re-expressed data appear similarly in Table 5-3.

Table 5-3 — Average Target Density Values Calculated From Table 5-1

Mission	Camera	D_{min}	D_{max}
1103-1	FWD	0.68	1.02
1103-1	AFT	0.74	1.02
1103-2	FWD	0.57	1.01
1103-2	AFT	0.66	0.95

Paired values of D_{min} and D_{max} for each specimen tracing in Table 5-1 were combined to produce density differences (ΔD). This makes it possible to characterize the contrast of the high priority target images on the 3404 original negative mode in a quantitative way. FWD and AFT coverage of each target were then compared by taking the ratio of their respective density differences. The two essential distinctions between the FWD and AFT cameras in this comparison are viewing aspect and spectral modification due to filtration. These distinctions are represented by identifying the filter employed in the image acquisition. Resultant data are presented in Table 5-4 in a format which basically tells how much more contrast one filter record has over its companion filter record for the same target coverage. For the purpose of graphic display, these data are grouped to illustrate their characteristic tendencies.

* Evaluation Report of Original Negatives, Mission 1103, Section II Density/Luminance (C-38-200590).

Table 5-4 — Filter Comparison With Regard to Target ΔD

W-25 and SF-05 (FWD Primary and AFT Alternate)		W-25 and W-21 (FWD Primary and AFT Primary)	
Target No.	ΔD Ratio	Target No.	ΔD Ratio
112	W-25 = 2.60 SF-05		
302	W-25 = 1.71 SF-05		
120	W-25 = 1.89 SF-05		
104	W-25 = 1.87 SF-05	257	W-25 = 1.05 W-21
31	W-25 = 1.06 SF-05	119	W-25 = 1.19 W-21
109	W-25 = 1.60 SF-05	714	W-25 = 1.17 W-21
116	W-25 = 1.76 SF-05	113	W-25 = 1.08 W-21
118	W-25 = 1.39 SF-05	801	W-25 = 1.06 W-21
223	W-25 = 1.74 SF-05	41	W-25 = 1.03 W-21
225	W-25 = 1.82 SF-05		
252	W-25 = 2.00 SF-05		
121	W-25 = 1.62 SF-05	256	W-25 = 1.00 W-21
123	W-25 = 1.66 SF-05		
16	W-25 = 2.63 SF-05		
101	W-25 = 2.12 SF-05	117	W-21 = 1.27 W-25
108	W-25 = 1.78 SF-05	229	W-21 = 1.25 W-25
209	W-25 = 1.60 SF-05	302	W-21 = 1.12 W-25
301	W-25 = 2.04 SF-05	112	W-21 = 1.16 W-25
36	W-25 = 1.52 SF-05	850	W-21 = 1.06 W-25
511	W-25 = 1.11 SF-05		
512	W-25 = 1.64 SF-05		
303	W-25 = 1.16 SF-05		
802	W-25 = 2.03 SF-05		
124	W-25 = 1.07 SF-05		

In making ΔD comparisons with the mission 1103 density analysis data as presented in Table 5-4, two tendencies emerge with regard to recorded target contrast on film Type 3404 through the three filters—W-25, W-21, and SF-05. The first is that the W-25 record generally exhibits 1.5 to 2.5 times greater contrast than the SF-05 record, as shown in the left column. Secondly, the W-25 and W-21 records are generally about equivalent in ΔD; their superiority with this criterion varies one over the other limited to a difference of up to only 1.2 times, as shown in the right column.

Comparison of the target and terrain average density thresholds as they appear in Tables 5-2 and 5-3 reveals that the target values define a narrower range contained within the wider range specified by the terrain values. Although the sample size for the target measurements is much smaller than that for the terrain measurements, the results are consistent for each of the four portions of the 1103 mission and this lends credence to accepting this effect as generally true.

In principle, a ΔD range would be greater for the smaller sampling aperture (10 microns as compared to 0.5 millimeter) because there would be less integration taking place. In the case under consideration, however, this relationship does not hold. Explanation of this reversal is supplied by the fact that the 10-micron diameter scanning aperture and the 0.5-millimeter random sampling aperture produce two different kinds of density due to the differences in the optical systems. However, the microdensitometer traces were calibrated on macro-step tablets for the exact purpose of correlating with the 0.5-millimeter densities. It remains to conclude that the densities listed in Tables 5-2 and 5-3 can be compared legitimately. In so doing, the average target density difference is contained within the average terrain density difference. This tendency is not consonant, however, with the larger body of data available in Project Sunny, wherein the average target ΔD is equal to the average terrain ΔD but shifted up into a higher density level.

The processing contractor has defined tolerance limits on both the toe and shoulder of the processing curves by the 1.2 gradient point. Their analysis concludes that a majority (52.6 percent) of the frames were underexposed and that, within each segment, AFT camera records were significantly less underexposed than were the FWD-camera records. This contractor's analysis of the exposure situation based on the high priority targets concludes that exposure was close to an optimum situation for the intelligence targets studied. This acquisition accuracy is attributed to the fact that the mission 1103 exposure value curves were purposefully weighted 0.3 stop less than the 1102 and 1101 mission curves, based on the target/terrain exposure analysis referenced on page 5-1.

6. RECOMMENDATIONS

The following recommendations are offered concerning future missions of the 1100 series panoramic camera systems.

1. The SO-230 or SO-205 films should replace the 3404 film as soon as possible. The faster emulsion incorporated in the SO-230 film and its ultrathin base counterpart, SO-205, would virtually eliminate image smear as a significant degrading factor of image quality.

2. Very careful consideration should be given to the advantages of using the SF-05 filter, since it would, by necessity, replace one of the Wratten filters that might have been utilized otherwise.

3. Two Wratten filters should be mounted on the filter tray of each panoramic camera. In the FWD-looking camera, a W-25 and a W-23A or a W-21 filter should be mounted. In the AFT-looking camera, a W-21 and a W-23A or W-25 filter should be mounted. For a specific target or a group of targets (during the mission), one of the two Wratten filters should be selected on the basis of known weather and haze conditions prevailing over the targets.

4. Since only a few CORN targets are deployed and photographed in each mission, special filter experiments should be avoided when the CORN targets are being photographed. CORN targets should be photographed with the primary filters: W-21 for the AFT-looking camera and W-25 for the FWD-looking camera. Whenever the requirement for special tests exists, additional CORN targets should be deployed to accommodate them.

5. The average altitude of photography for the HPL targets should be reduced to 80 nm.

6. Occasionally some very large V/h programming errors have been observed. It should be possible to reduce all V/h programming errors to less than 1.5 percent.

7. The air-to-vacuum focus shift of each lens should be determined photographically by performing static resolution tests in the small vacuum chamber.

8. For each camera, dynamic resolution versus focus tests with various amounts of IMC mismatch should be performed in order to obtain data which will allow correct focussing of the camera.

9. If it is desirable to utilize an SF-05 filter in a panoramic camera, the specific filter and panoramic camera should be thoroughly tested together in the laboratory before a final decision is reached about the operational use of that SF-05 filter in one of the future missions.

Appendix A

RESOLUTION PREDICTIONS FOR CORN TARGETS

This appendix is a listing of the image smear and resolution data which have been computed for the CORN targets (see Tables A-1 and A-2).

Notation

BALTR = image smear, along track, random, microns
BALTS = image smear, along track, systematic, microns
TBAT = total blur, along track, microns
RESL = dynamic film resolution, along track, low contrast (2:1), lines per millimeter
RESH = dynamic film resolution, along track, high contrast, lines per millimeter
GDRL = ground resolution, along track, low contrast, feet
GDRH = ground resolution, along track, high contrast, feet
BCTR = image smear, cross track, random, microns
BCTS = image smear, cross track, systematic, microns
TBCT = total image smear, cross track, microns
CRESL = dynamic film resolution, cross track, low contrast, lines per millimeter
CRESH = dynamic film resolution, cross track, high contrast, lines per millimeter
CGDRL = ground resolution, cross track, low contrast, feet
CGDRH = ground resolution, cross track, high contrast, feet

Table A-1 — Resolution Predictions for CORN Targets, FWD-Looking Camera, Unit No. 307

Pass	16	97
Frame	7	7
Along Track		
BALTR	2.03	2.05
BALTS	2.71	-0.14
TBAT	4.74	2.19
RESL	113.4	133.5
RESH	149.5	212.6
GDRL	8.6	7.0
GDRH	6.5	4.4
Cross Track		
BCTR	0.61	0.61
BCTS	0.40	4.51
TBCT	1.01	5.12
CRESL	136.4	127.1
CRESH	216.3	150.1
CGDRL	6.9	7.2
CGDRH	4.3	6.1

Table A-2 — Resolution Predictions for CORN Targets, AFT-Looking Camera, Unit No. 306

Pass	16	16	97	97
Frame	13	21	13	20
Along Track				
BALTR	1.43	1.68	1.34	1.33
BALTS	-1.80	-1.42	-0.85	0.52
TBAT	3.23	3.11	2.19	1.85
RESL	123.2	127.2	132.2	134.3
GDRL	7.8	7.7	6.9	7.1
Cross Track				
BCTR	0.43	0.51	0.40	0.39
BCTS	0.58	3.43	3.93	4.24
TBCT	1.01	3.94	4.33	4.63
CRESL	130.4	122.3	120.4	118.9
CGDRL	7.1	7.7	7.5	7.9

Appendix B

RESOLUTION PREDICTIONS FOR HPL TARGETS

Resolution predictions for HPL targets are contained in Tables B-1 and B-2. Table B-3 contains average low contrast ground resolution versus photointerpreter rating data.

Table B-1 — Resolution Predictions for HPL Targets, FWD-Looking Camera, Unit No. 307

Target	120	112	104	229	109	31
Pass	7	8	24	25	39	39
Frame	13	6	138	8	46	117
Along Track						
BALTR	2.02	2.00	1.93	2.02	2.06	2.09
BALTS	1.36	0.17	2.32	0.33	0.17	0.16
TBAT	3.38	2.17	4.25	2.35	2.23	2.18
RESL	122.6	125.3	105.2	124.8	126.0	125.2
RESH	178.7	202.9	138.8	203.2	209.1	204.7
GDRL	8.7	8.8	10.2	8.0	8.0	7.8
GDRH	6.0	5.4	7.8	4.9	4.8	4.8
Cross Track						
BCTR	0.60	0.59	0.56	0.60	0.62	0.60
BCTS	4.32	5.38	5.31	-0.28	2.47	4.63
TBCT	4.92	5.97	5.88	0.88	3.09	5.23
CRESL	120.6	112.1	104.5	141.5	135.5	118.4
CRESH	150.2	130.9	120.8	221.6	185.1	142.4
CGDRL	8.7	9.8	10.5	6.9	7.2	8.1
CGDRH	7.0	8.4	9.1	4.4	5.3	6.8

Table B-1 — Resolution Predictions for HPL Targets, FWD-Looking Camera, Unit No. 307 (Cont.)

Target	117	116	302	256	257	118
Pass	55	71	72	88	105	106
Frame	8	5	8	47	8	6
Along Track						
BALTR	2.09	2.08	1.98	1.84	2.10	1.80
BALTS	−0.45	0.63	−0.43	0.81	−1.62	0.92
TBAT	2.54	2.70	2.41	2.65	3.72	2.72
RESL	126.9	127.1	121.8	125.6	122.5	128.8
RESH	195.4	196.1	202.6	197.9	176.6	191.7
GDRL	7.8	7.9	8.1	8.4	7.5	8.8
GDRH	5.0	5.1	4.9	5.4	5.2	5.9
Cross Track						
BCTR	0.63	0.62	0.58	0.53	0.63	0.51
BCTS	2.69	0.06	−2.85	6.72	2.04	7.30
TBCT	3.32	0.68	3.43	7.24	2.67	7.81
CRESL	132.6	142.7	127.9	105.4	142.1	101.0
CRESH	175.4	237.9	171.8	117.1	193.2	110.9
CGDRL	7.2	6.8	7.8	11.0	6.3	12.5
CGDRH	5.4	4.1	5.8	9.9	4.6	11.4

Table B-1 — Resolution Predictions for HPL Targets, FWD-Looking Camera, Unit No. 307 (Cont.)

Target	223	225	252	123	121	714
Pass	106	106	106	121	121	134
Frame	25	34	36	118	134	11
Along Track						
BALTR	2.04	2.10	2.08	1.92	2.03	2.05
BALTS	−0.90	−0.85	0.40	0.62	0.92	−1.50
TBAT	2.94	2.95	2.48	2.54	2.95	3.55
RESL	121.8	122.7	128.9	126.9	124.4	120.9
RESH	184.9	188.6	204.0	197.3	190.7	179.6
GDRL	8.0	7.5	7.4	8.2	7.8	7.7
GDRH	5.2	4.9	4.7	5.3	5.1	5.2
Cross Track						
BCTR	0.60	0.63	0.63	0.56	0.60	0.61
BCTS	−1.60	2.56	3.26	6.01	−0.69	4.73
TBCT	2.21	3.19	3.88	6.56	1.29	5.34
CRESL	131.6	131.7	132.7	110.1	142.8	119.9
CRESH	193.0	178.9	175.4	124.3	223.9	142.8
CGDRL	7.4	6.8	6.9	9.8	6.7	7.8
CGDRH	5.0	5.0	5.2	8.7	4.3	6.5

Table B-1 — Resolution Predictions for HPL Targets, FWD-Looking Camera, Unit No. 307 (Cont.)

Target	113	801	124	16	101	108
Pass	138	138	153	154	154	154
Frame	45	48	28	4	17	38
Along Track						
BALTR	1.96	2.00	1.99	3.17	3.10	2.92
BALTS	−2.74	−0.67	−0.31	− 2.52	− 2.00	−1.81
TBAT	4.70	2.67	2.30	5.70	5.10	4.73
RESL	121.6	130.8	124.9	109.6	112.6	115.4
RESH	157.2	202.7	200.2	138.8	148.2	155.5
GDRL	8.2	7.7	7.9	8.8	8.7	8.8
GDRH	6.4	5.0	4.9	7.0	6.6	6.6
Cross Track						
BCTR	0.57	0.58	0.58	0.95	0.93	0.85
BCTS	5.93	−4.07	− 2.56	1.58	5.27	−8.75
TBCT	6.51	4.65	3.15	2.53	6.20	9.60
CRESL	110.9	130.0	130.3	133.1	109.5	88.4
CRESH	127.1	202.7	178.7	193.0	128.8	93.0
CGDRL	9.5	7.7	7.7	7.1	8.8	12.1
CGDRH	8.3	5.0	5.6	4.9	7.5	11.5

Table B-1 — Resolution Predictions for HPL Targets, FWD-Looking Camera, Unit No. 307 (Cont.)

Target	301	209	119	302	41	850
Pass	154	154	167	169	183	183
Frame	92	134	12	63	5	15
Along Track						
BALTR	1.88	1.88	1.93	1.89	1.82	1.98
BALTS	0.14	0.31	-1.69	-1.39	-1.91	-0.56
TBAT	2.02	2.19	3.62	3.28	3.73	2.54
RESL	126.6	131.7	120.6	121.3	127.8	124.2
RESH	210.1	313.2	177.6	180.2	177.2	195.5
GDRL	8.2	7.9	8.3	8.4	7.8	7.5
GDRH	5.0	4.9	5.7	5.7	5.7	4.8
Cross Track						
BCTR	0.54	0.54	0.56	0.54	0.51	0.58
BCTS	6.52	-7.53	6.32	6.82	7.07	5.59
TBCT	7.06	8.07	6.88	7.36	7.58	6.17
CRESL	105.2	101.5	107.7	102.4	102.6	110.7
CRESH	117.6	109.0	120.5	113.6	112.4	128.2
CGDRL	10.6	11.0	9.9	10.9	11.0	8.7
CGDRH	9.5	10.3	8.9	9.8	10.1	7.5

Table B-1 — Resolution Predictions for HPL Targets, FWD-Looking Camera, Unit No. 307 (Concl.)

Target	36	511	512	303	802	112
Pass	184	200	200	200	203	218
Frame	10	5	8	8	21	13
Along Track						
BALTR	3.06	2.09	2.00	2.09	3.06	3.05
BALTS	-34.91	0.09	-0.04	0.19	1.27	1.02
TBAT	37.98	2.18	2.04	2.28	4.33	4.07
RESL	27.4	130.8	129.4	127.7	117.7	123.6
RESH	25.7	209.5	209.8	209.9	165.2	168.9
GDRL	35.5	6.9	7.3	7.1	7.9	7.6
GDRH	37.9	4.3	4.5	4.3	5.6	5.6
Cross Track						
BCTR	0.89	0.63	0.59	0.63	0.92	0.92
BCTS	-8.77	2.37	-2.75	1.09	0.45	2.20
TBCT	9.66	2.99	3.34	1.71	1.37	3.12
CRESL	86.3	141.8	136.4	147.3	142.6	132.9
CRESH	91.8	191.3	180.4	223.2	219.2	183.9
CGDRL	11.6	6.1	7.0	5.9	6.4	6.9
CGDRH	10.9	4.5	5.3	3.9	4.2	5.0

Table B-2 — Resolution Predictions for HPL Targets, AFT-Looking Camera, Unit No. 306

Target	112	229	117	302	256	257
Pass	8	25	55	72	88	105
Frame	12	14	14	14	53	14
Along Track						
BALTR	1.30	1.33	1.38	1.31	1.23	1.38
BALTS	0.27	0.38	−0.42	0.01	−1.57	0.16
TBAT	1.57	1.72	1.80	1.32	2.80	1.54
RESL	133.3	125.3	127.0	123.1	130.4	133.3
GDRL	8.2	7.9	7.7	8.0	7.9	7.0
Cross Track						
BCTR	0.39	0.40	0.42	0.38	0.35	0.42
BCTS	6.33	−0.84	2.28	−2.81	5.63	2.74
TBCT	6.71	1.24	2.70	3.20	5.99	3.16
CRESL	102.5	126.2	124.0	117.6	108.8	126.9
CGDRL	10.8	7.8	7.7	8.5	10.5	7.1

Table B-2 — Resolution Predictions for HPL Targets, AFT-Looking Camera, Unit No. 306 (Cont.)

Target	714	113	801	119	41	850
Pass	134	138	138	167	183	183
Frame	17	51	54	18	11	21
Along Track						
BALTR	1.35	1.29	1.32	1.27	1.20	1.30
BALTS	-0.31	0.08	-1.23	-0.24	0.38	-0.46
TBAT	1.66	1.37	2.55	1.52	1.59	1.76
RESL	129.2	133.7	128.1	131.5	135.1	129.9
GDRL	7.3	7.8	7.7	7.8	7.7	7.2
Cross Track						
BCTR	0.40	0.38	0.39	0.37	0.34	0.38
BCTS	5.81	5.57	-3.54	6.17	5.42	6.39
TBCT	6.21	5.94	3.93	6.54	5.76	6.77
CRESL	104.3	108.2	120.9	103.0	110.5	100.9
CGDRL	9.0	10.0	8.5	10.5	10.4	9.5

Table B-3 — Average Low Contrast Ground Resolved Distance Versus Photointerpreter Ratings

The average low contrast ground resolved distance is obtained by averaging the ground resolved distances for the FWD- and AFT-looking cameras in both the along- and cross-track directions. In other words, it is the average of four numbers. Note that the photointerpreter ratings include weather effects which have been eliminated by necessity from the predicted average ground resolved distance.

Target	Pass	Average GRD, feet	Photointerpreter Rating
112	8	9.4	Fair
229	25	7.7	Fair
117	55	7.6	Fair
302	72	8.1	Fair
256	88	9.5	Fair
257	105	7.0	Fair
714	134	8.0	Fair
113	138	8.9	Fair
801	138	7.9	Fair
119	167	9.1	Fair
41	183	9.2	Fair
850	183	8.2	Good

The following cumulative statistics have been computed for the various photointerpreter ratings. These statistics include the photointerpreter ratings and predicted average GRD's of missions 1101, 1102, and 1103.

Photointerpreter Rating	Mean GRD, feet	Standard Deviation, feet
Good	10.0	2.6
Fair	11.3	2.9
Poor	17.1	4.1

Appendix C

PHOTOGRAPHIC ILLUSTRATIONS

Photographic illustrations are included in this report to show the quality of the best photography from this mission relative to the best photography from the two preceding KH-4B missions. Comparative photomicrographs (at approximately 100×) made from the MIP frames of missions 1101, 1102 and 1103 are presented on the next page. The mission 1103 sample is comparable to the mission 1101 sample, both having an MIP rating of 95. The mission 1102 sample is rated slightly higher at MIP 100.

Each of these selected frames were produced with different filter/slit combinations during different seasons of the year, as shown in Table C-1.

Table C-1 — Ephemeral Information for the MIP Frames Under Consideration

Mission	Filter	Slit Width, inches	Month	Solar Altitude
1101	W-23A	0.218	September (1967)	43° 04'
1102	W-25	0.340	December (1967)	34° 34'
1103	W-25	0.195	May (1968)	63° 02'

NOTE: That all three MIP frames were chosen from FWD-looking camera acquisitions.

[redacted]

~~TOP SECRET~~

~~NO FOREIGN DISSEMINATION~~

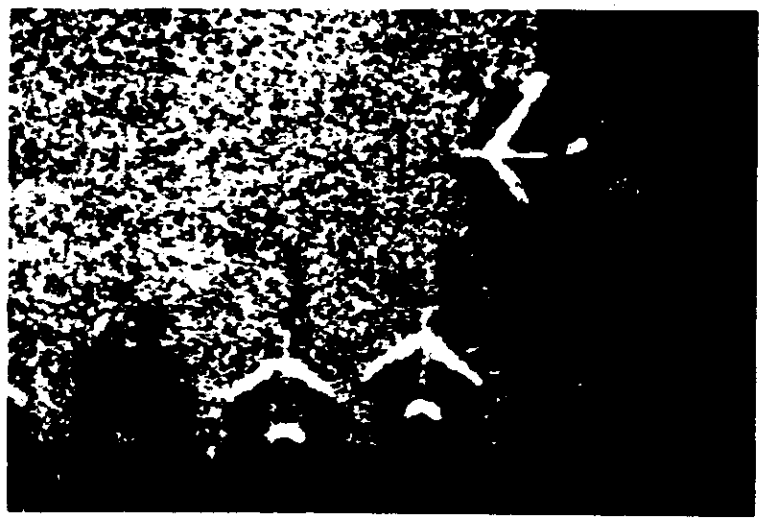

MIP Frame
Mission—1101-2
Pass—D159
Camera—Fwd
Frame—002
Altitude—84 nm
X-Coord—39.0
System—KH-4B
MIP 95

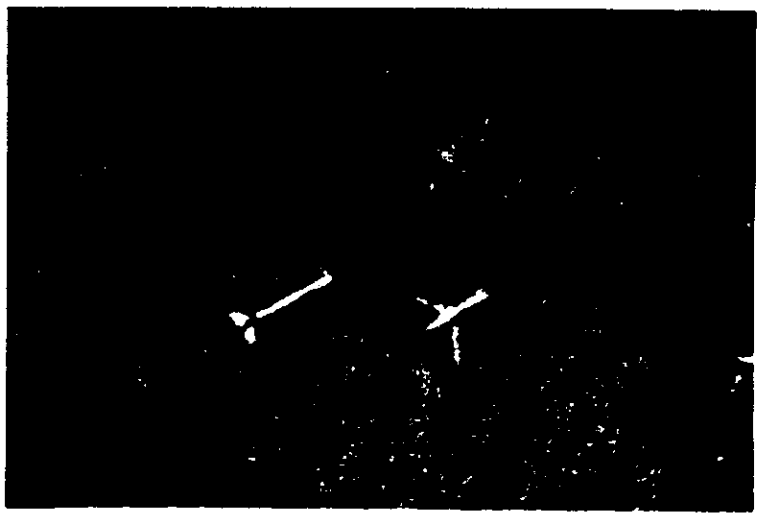

MIP Frame
Mission—1102-1
Pass—D016
Camera—Fwd
Frame—022
Altitude—88 nm
X-Coord—26.8
System—KH-4B
MIP 100

MIP Frame
Mission 1103-1
Pass—D079
Camera—Fwd
Frame—015
Altitude—86.5 nm
X-Coord—41.0
System—KH-4B
MIP 95

100× (Approx) Photomicrographs from MIP Frames of Missions 1101, 1102, and 1103

~~TOP SECRET~~

~~NO FOREIGN DISSEMINATION~~

~~HANDLE VIA~~
~~TALENT-KEYHOLE~~
~~CONTROL SYSTEM ONLY~~

Appendix D

WEATHER ASSESSMENT

In a continuing effort to evaluate the impact of weather (principally haze) on main camera performance, all DISIC frames having corresponding main camera photography have been evaluated. This evaluation involves determining for each frame the percent of frame area that is cloudy, clear, or hazy. If the amount that each of these three conditions represents in the format is known, the haze ratio (an area weighted percentage of haze in the cloud-free portions of the format) can be determined.

The data in Table D-1 represent the average weather assessment for all DISIC frames in both segments of mission 1103. The data in Table D-2 are a pass-by-pass weather estimate of the entire 1103 mission. In Table D-3, the averages of this mission are compared with results obtained from the two previous 1100 series missions. There appear to be no substantial differences in the data for these missions.

Table D-1' — Weather Estimate Averages for the Entire Panoramic Coverage Portion of the Mission

Mission	Cloud, percent	Clear, percent	Haze, percent	Haze Ratio
1103-1	35.3	49.8	14.8	22.9
1103-2	32.3	57.8	9.9	14.6
Mission Average	33.8	53.8	12.4	18.8

Table D-2 — Weather Estimate Mission 1103-1

Pass	Cloud, percent	Clear, percent	Haze, percent	Haze Ratio	Pass	Cloud, percent	Clear, percent	Haze, percent	Haze Ratio
D-001	75	—	25	100	D-061	—	100		
D-003	—	62.0	38	38	D-063	77.5	22.5	—	—
D-005	100	—	—	—	D-064	100	—	—	—
D-006	73.7	20	6.3	23.9	D-071	5	88.7	6.3	6.6
D-007	21.2	78.8	—	—	D-072	15	35	50	58.8
D-008	—	100	—	—	D-073	—	100	—	—
D-009	44	—	56	100	D-074	—	100	—	—
D-010	53.3	46.7	—	—	D-076	63.3	35	1.7	4.6
D-014	1.7	98.3	—	—	D-079	3.3	93.4	3.3	3.4
D-016	40	60	—	—	D-085	5	95	—	—
D-021	70	29	1	3	D-086	43.3	56.7	—	—
D-022	26.7	73.3	—	—	D-087	62.2	36.9	0.9	2.4
D-023	55.4	44.6	—	—	D-088	63.3	16.7	20	54.4
D-024	32.6	50.2	17.2	25.5	D-089	15.3	30	54.7	64.6
D-025	23.9	60	16.1	21.2	D-090	24.2	71.6	4.2	5.5
D-032	7.5	87.5	5	5.4	D-097	55	45	—	—
D-037	37.6	59	3.4	5.4	D-102	—	100	—	—
D-038	43.8	—	56.2	100	D-103	48.6	—	51.4	100
D-039	50.9	36.8	12.3	25	D-104	60	25.6	13.4	33.5
D-040	54.4	45.6	—	—					
D-041	12	62	26	29.5					
D-042	55.7	35.7	8.6	19.4		Mission Average			
D-048	46.6	53.4	—	—					
D-052	—	20	80	80		Cloud	Haze	Clear	Haze Ratio
D-054	53.2	37.4	9.4	20					
D-055	—	100	—	—		35.4%	49.8%	14.8%	22.9
D-057	45.4	48.5	6.1	11.2					
D-058	7.7	85.4	6.9	7.5					

Table D-3 — Comparison of Final Averages Obtained From Missions 1101, 1102 and 1103

Mission	Cloud, percent	Clear, percent	Haze, percent	Haze Ratio	NPIC Evaluation, percent
1101-1	33	52.5	14.5	21.6	65
1101-2	33	58.5	8.5	12.7	70
1102-1	30.1	58.4	11.5	16.4	70
1102-2	32.7	50.4	16.9	25.1	75
1103-1	35.4	49.8	14.8	22.9	
1103-2	32.3	57.8	9.9	14.6	
Mean Average					
1101	33	55.5	11.5	17.1	
1102	31.4	54.4	14.2	20.8	
1103	33.8	53.8	12.4	18.8	

Appendix E

ANALYSIS OF DRT PHOTOGRAPHIC TESTS ON SYSTEM 1109

1. DESCRIPTION OF TESTS

Several photographic tests were run on instruments no. 316 and 317 in the contractor's DRT facility. This facility consists of a large vacuum chamber which will take a complete panoramic system. Outside the chamber a 200-inch-effective-focal-length collimator and a target wheel allow photographic resolution tests (including simulated image motion tests) to be run on an instrument by controlling the angular (V/h) rate of the resolution targets mounted on the target wheel. A window on the chamber allows one to run these tests with an instrument inside the chamber under vacuum conditions.

The tests that were run utilized high contrast targets on the target wheel and ultra-thin-base SO-380 film in the instruments.

The purpose of the tests was to examine the performance of the lenses at various focal positions and to evaluate the air-to-vacuum focus shift behavior of the lenses. The intention was to use the information obtained from the DRT tests towards understanding and possibly solving the focus difficulties of the 1100 series systems.

The individual tests and the results of their analysis are described below.

Groups No. 2 and 4

Group no. 2 of the tests is a through-focus test of instrument no. 316 (lens I-195) in steps of 0.0005 inch of focus position conducted in vacuum. The resulting resolution through-focus-position curve (average of along- and cross-track directions) is plotted in Fig. E-1. The same figure shows the corresponding resolution versus focus curve obtained at ETL* in air and assuming an air-to-vacuum focus shift of 0.014 inch. From film-lift tests we have established that the film lift above the focal plane rollers in the DRT chamber was on the average 0.0006 inch higher than the corresponding film lift at ETL. The differences in the curve shapes shown in Figs. E-1 and E-2 should be attributed to differences in collimator performance between the 120-inch collimator at ETL and the 200-inch collimator at DRT. Thus, in order to relate the ETL curve to the DRT curve, the portions of the curves below a resolution level of 180 lines per millimeter were utilized. The relative positions of the ETL and DRT curves in Fig. E-1, the assumed air-to-vacuum focus shift of 0.014 inch, and the difference in film lift between the two locations implies that the actual air-to-vacuum focus shift for lens I-195 is 0.0133 inch.

---

*Environmental Test Laboratory (the 1100 series panoramic cameras are all tested in this laboratory).

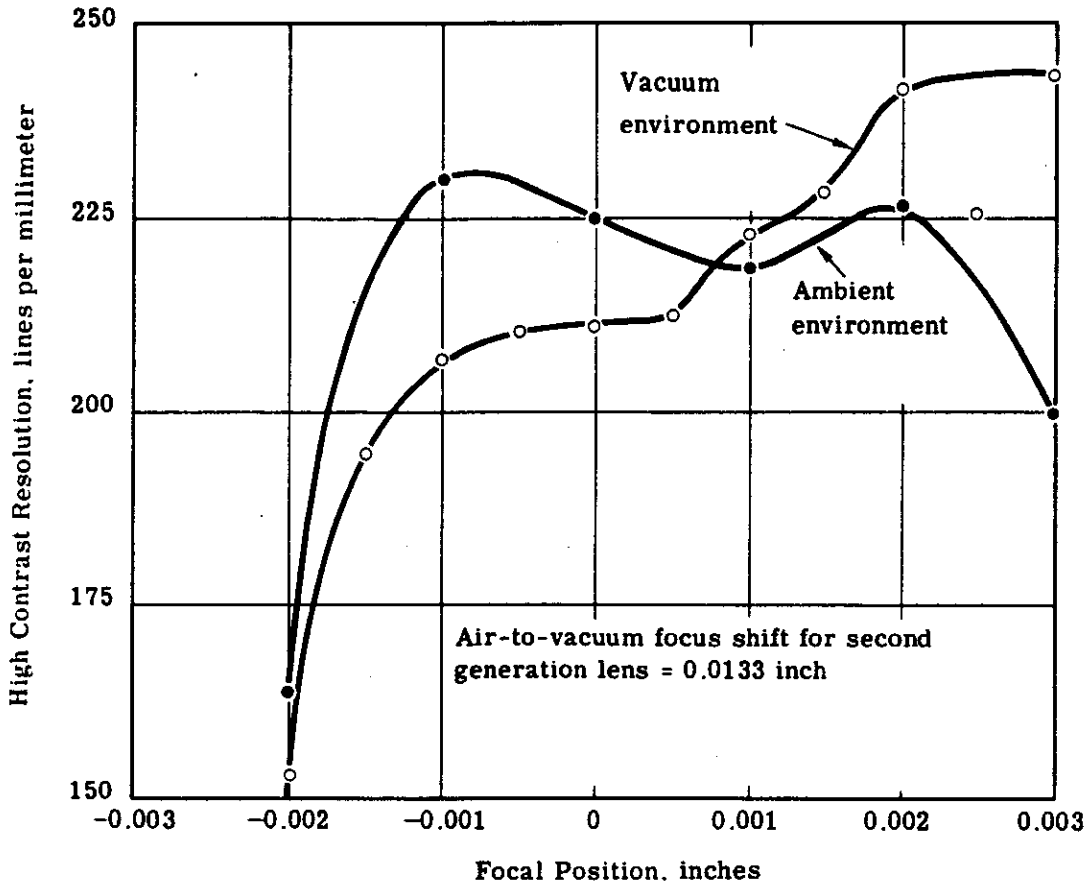

Fig. E-1 — Comparative dynamic resolution through-focus tests on unit no. 316

Groups No. 11 and 14

Groups no. 11 and 14 of the tests are identical to groups no. 2 and 4 discussed above except they were performed on instrument no. 317 (lens I-200). The results of these tests are shown in Fig. E-2. Again, it was established that the film lift for instrument no. 317 at the DRT chamber was 0.0007 inch higher (on the average) than the film lift at ETL. The relative positions of the ETL and DRT curves in Fig. E-2, the assumed air-to-vaccum focus shift of 0.014 inch, and the difference in film lift between the two locations implies that the actual air-to-vacuum focus shift for lens I-200 is 0.0146 inch.

Group No. 13

Group no. 13 is a through focus test of instrument no. 317 in the DRT chamber conducted in air and assuming a 0.014-inch air-to-vacuum focus shift. This test gave very erratic results for unknown reasons. The air-to-vacuum focus shift cannot be determined from this test.

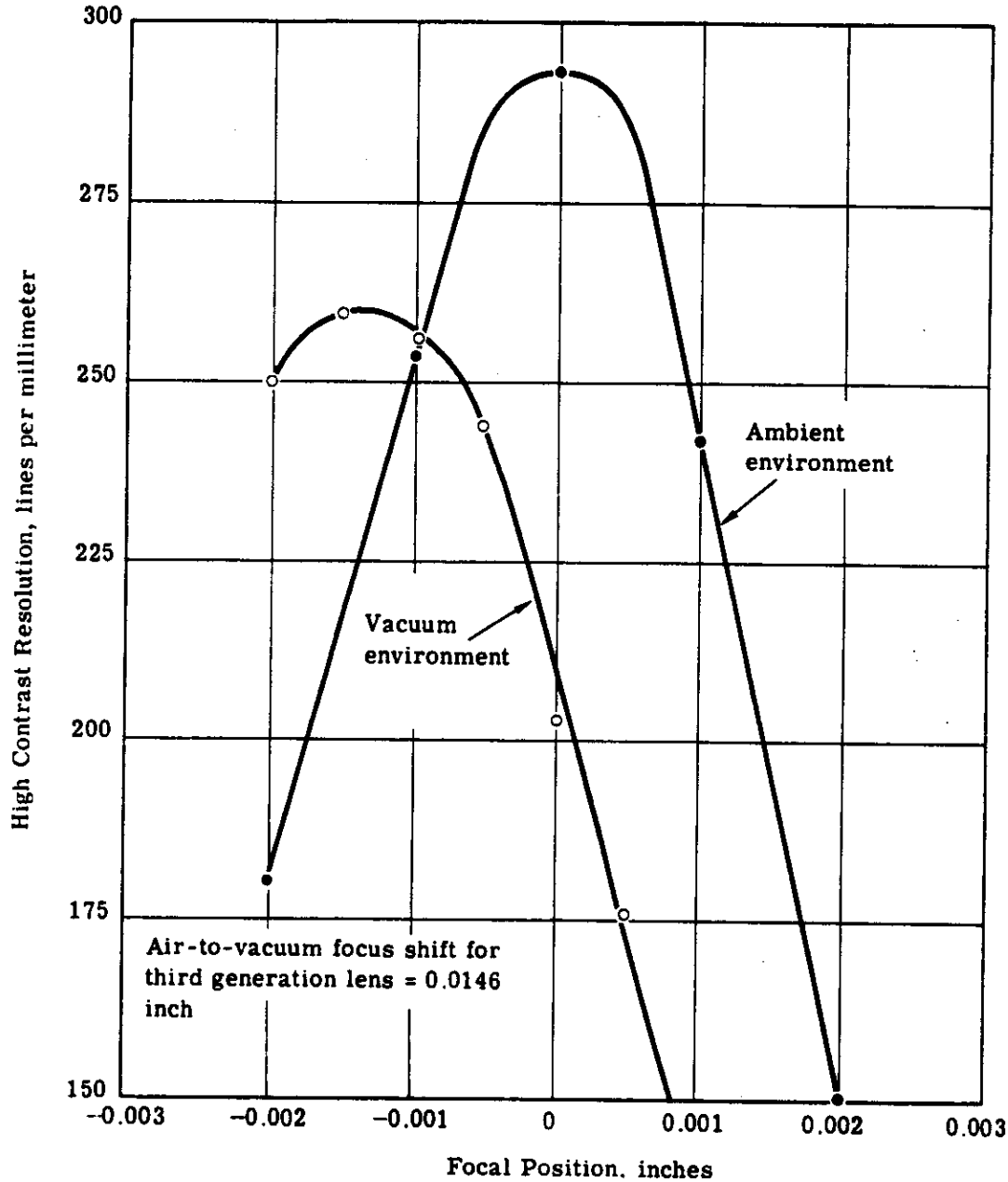

Fig. E-2 — Comparative dynamic resolution through-focus tests on unit no. 317

Group No. 12

Group no. 12 is a sequence of tests on instrument no. 317 in vacuum during which the focal position was varied in 0.0005-inch steps and the IMC mismatch between the target wheel and the instrument was varied in steps of 5 percent. The results of these tests are shown in Fig. E-3. Examination of Figs. E-2 and E-3 shows that the 0 percent IMC mismatch curve reaches its peak at the −0.0012-inch focus position. However, as the percent of IMC mismatch increases (IMC mismatch is equivalent to introducing image smear in the IMC direction with 5 percent of IMC mismatch corresponding to 2.3 microns of smear), the peak focus shifts to the −0.0005-inch focus position and finally to the 0.000 focus position. Since, operationally, the instrument is expected to experience about 3 microns of image smear in addition to about 2 microns of smear present under laboratory testing conditions, one expects the operational peak resolution performance to occur at approximately −0.0004 inch (see Fig. E-3). In other words, it appears that the operational peak focus for high contrast targets is displaced 0.0008 inch from the laboratory peak focus (high contrast) farther away from the field flattener. The implication is that if one desires to establish the operational peak focus position, one should run a through-focus test with about 7.5 percent IMC mismatch.

In addition, the curves of Fig. E-3 reveal some important facts about the behavior of the lens MTF at various focus positions. Assume that the MTF's of the lens at the three focus positions −0.001, −0.0005, and 0.000 were available. When a through focus test is run with a certain IMC mismatch, the three MTF's are all multiplied by the same (sin x/x) function, which is the Fourier transform of the corresponding image smear. The focus position which produces the maximum resolution must correspond to an MTF whose modulation at the resolution frequency is higher than the modulations of the MTF's associated with the other two focus positions. If the three MTF's did not intercept each other at any frequency other than 0 and the lens cut-off frequency, then the peak resolution in a through-focus test would occur at the same focus position independent of the percentage of IMC mismatch. The fact that the peak focus shifts according to the amount of IMC mismatch (image smear) indicates that the three MTF curves intercept each other. In fact, from Fig. E-3 we can estimate the crossover frequencies of the three MTF's. The MTF's from the −0.001 and −0.0005 focus position intercept approximately at 240 lines per millimeter, and the MTF's from the −0.0005 and 0.000 focus positions intercept at about 185 lines per millimeter. Another interpretation of the MTF intercepts is that the peak focus position is dependent on spatial frequency. The high frequencies (higher than 240 lines per millimeter) focus about 0.001 or more inches closer to the field flattener than the low frequencies (lower than 185 lines per millimeter). This observation suggests that the lens may have a very small amount of spherical aberration which, in fact, has been independently confirmed by mathematical (computer) evaluations. These evaluations (for a third generation lens with a W-25 filter) have shown that:

1. The high contrast resolution reaches a peak about 0.0009 inch closer to the field flattener than the paraxial focus.
2. The low contrast (2:1) resolution reaches a peak about 0.0007 inch closer to the field flattener than the paraxial focus.
3. The rms spherical waveform distortion reaches a minimum at about 0.0003 inch closer to the field flattener than the paraxial focus.

We feel that these mathematical computations reinforce the experimental results which were discussed above.

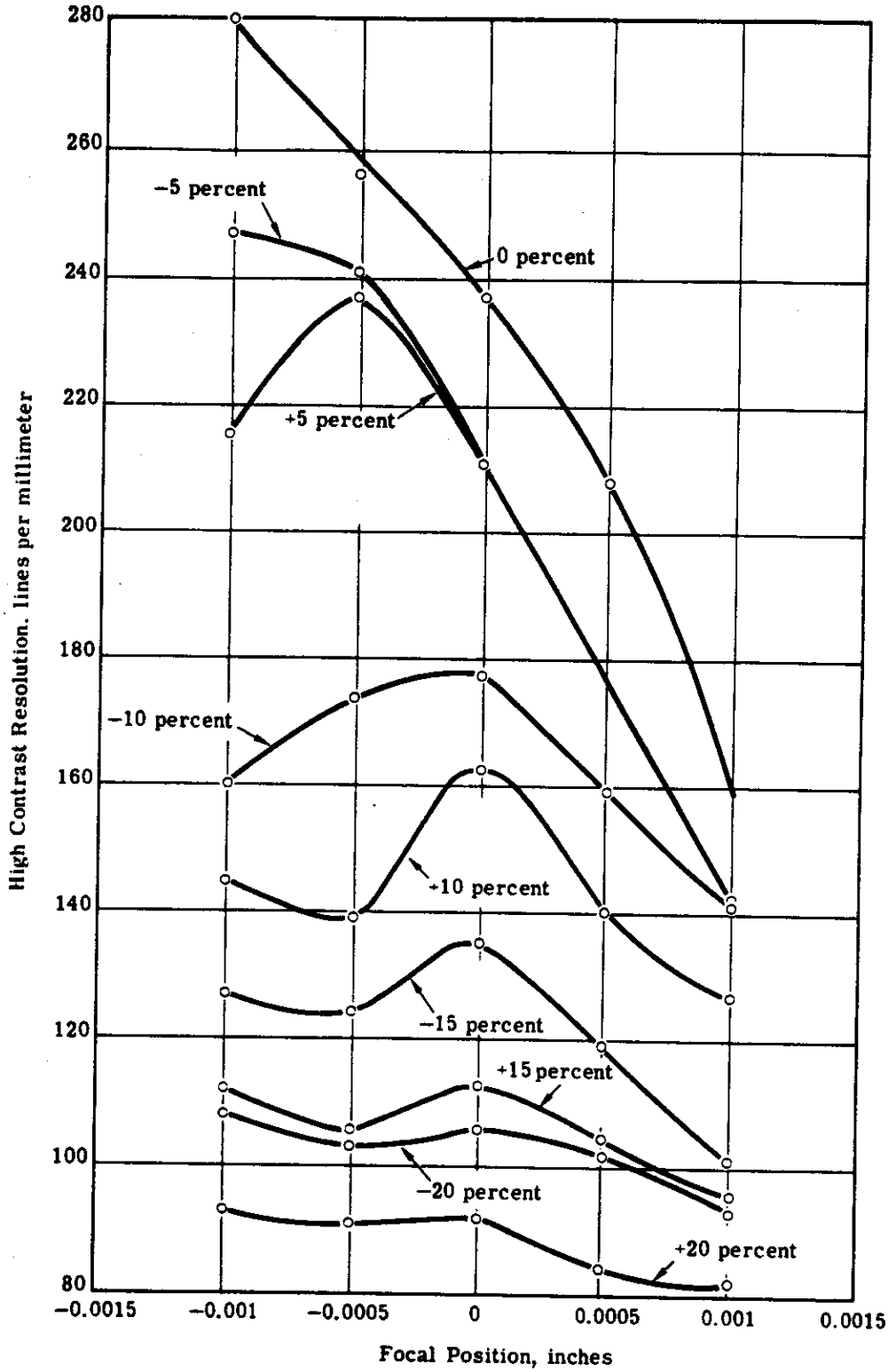

Fig. E-3 — Dynamic resolution through-focus tests on instrument no. 317 for different values of IMC mismatch

Group No. 3

Group no. 3 of the DRT tests were identical to the tests of group no. 12 except they were performed on instrument no. 316. The results were not as dramatic as in instrument no. 317 but they also indicated a focus shift of about 0.001 inch away from the field flattener as the IMC mismatch was increased.

A similar mathematical evaluation of a second generation lens (I-192) combined with a W-21 filter produced the following information:

1. The high contrast resolution reaches a peak about 0.0008 inch closer to the field flattener than the paraxial focus.
2. The low contrast (2:1) resolution reaches a peak about 0.0006 inch closer to the field flattener than the paraxial focus.
3. The rms spherical waveform distortion reaches a minimum at the paraxial focus within 0.0001 inch.

2. CONCLUSIONS

Unless one has specific reasons for favoring certain spatial frequencies, a Petzval lens should be focused so that the rms spherical waveform distortion is minimum, since at that point the lens performance comes closest to the performance of the theoretical diffraction-limited lens. One would have to determine experimentally the focus position at which the high contrast resolution reaches a peak. Then, the scan head should be shimmed accordingly so that the dynamic film position would coincide with the minimum rms distortion position, which is displaced by 0.0007 inch from the high contrast resolution peak, further away from the field flattener.

In addition, since the dynamic resolution tests will be performed in air, it is essential that the air-to-vacuum focus shift problem be clarified. Significant variations in the air-to-vacuum focus shifts (variations larger than 0.0003 inch) are not likely for lenses of the same generation. However, it seems possible that the second generation lenses may display an air-to-vacuum focus shift significantly different than the focus shift of the third generation lenses. The DRT and ETL tests discussed in paragraph 1 showed an air-to-vacuum focus shift of 0.0133 inch for lens I-195 (a second generation lens) and a corresponding focus shift of 0.0146 inch for lens I-200 (a third generation lens).

Appendix F

SPECIAL RESOLUTION TESTS ON SYSTEM 1105

Special resolution tests were run on the 1105 system. These were through-focus resolution tests on instruments no. 310 and 311 with various amounts of IMC mismatch. The focus was changed in increments of 0.0005 inch.

The film records were subsequently read by a resolution reader group.

The resolution readings were averaged by the recommended method of majority averaging (eliminating 10 percent of the highest readings and 40 percent of the lowest readings).

The results are shown in Figs. F-1, F-2, and F-3.

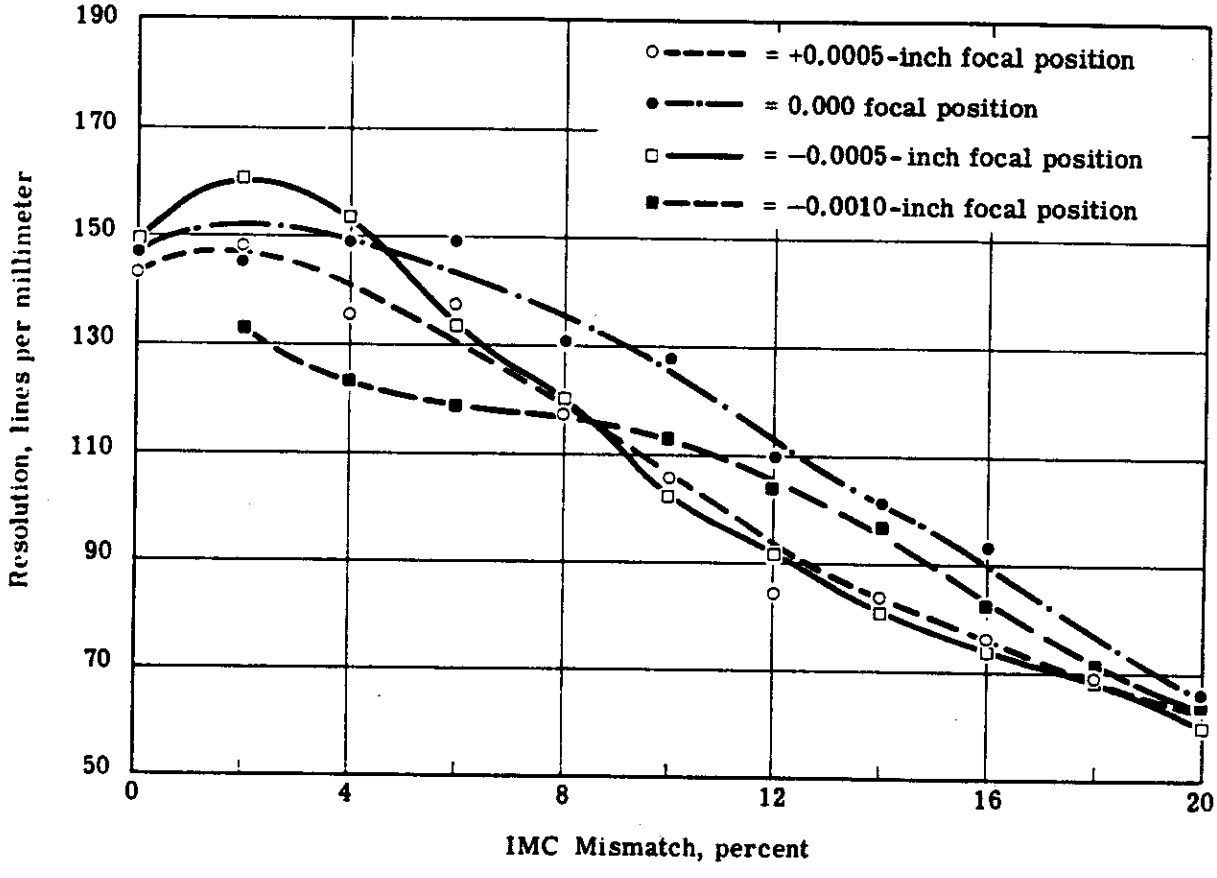

Fig. F-1 — Unit no. 310, low contrast resolution readings

All three figures show that the peaks of their curves appear at the +2 percent IMC mismatch position. This, then, must be the position of minimum smear (true 0 percent IMC mismatch) in the IMC direction. The corresponding target wheel speed must actually produce the best V/h synchronization between the instruments and the target wheel.

In Fig. F-1, the focal position identified as 0 should be the optimum focal position and produce the best photography. Another interesting observation in Fig. F-1 is that the focal position identified as −0.0005 inch actually produces the maximum low contrast resolution for less than approximately 4 percent IMC mismatch. This is in agreement with the observations and theoretical predictions discussed in Appendix E. One of the conclusions of this appendix is that the optimum lens focal position is located 0.0005 inch further away from the field flattener than the low contrast resolution peak.

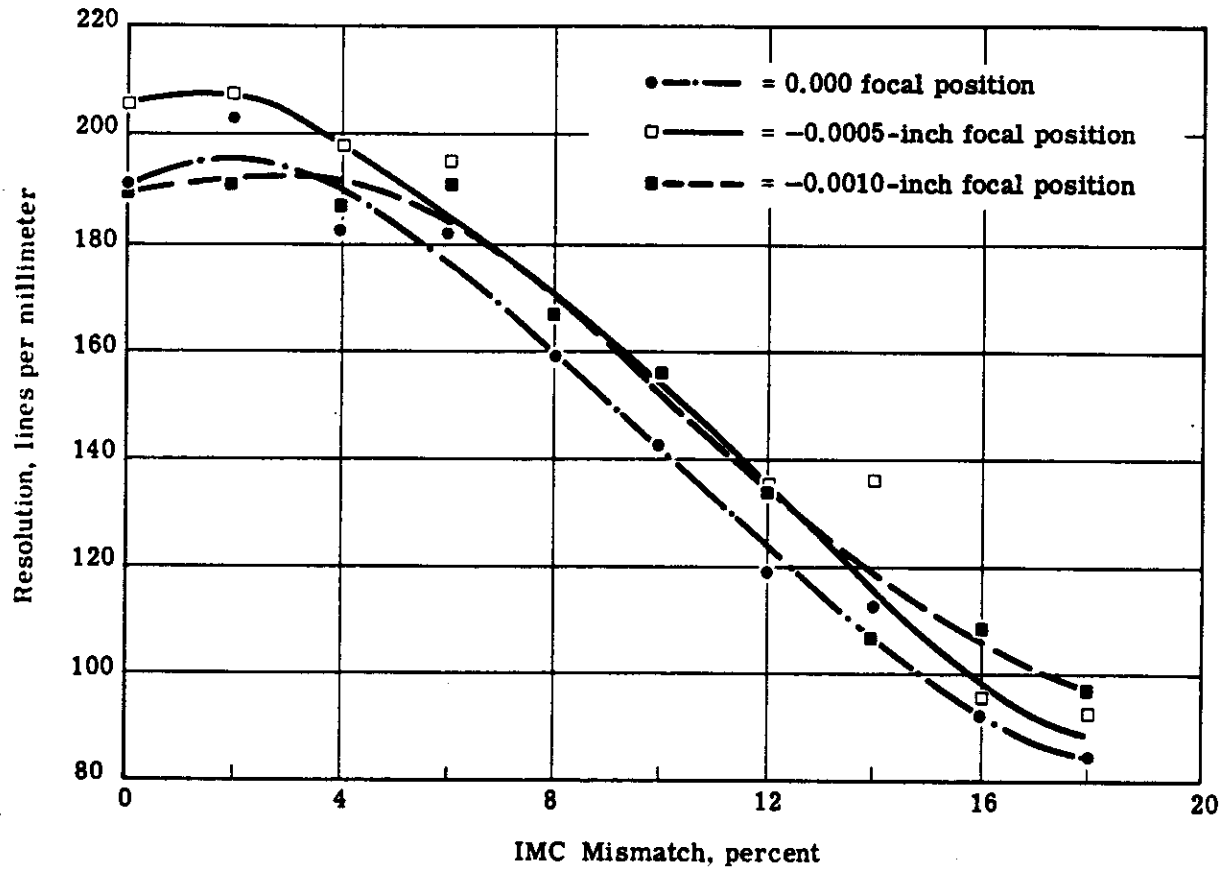

Fig. F-2 — Unit no. 311, low contrast resolution readings

It appears from Figs. F-2 and F-3 that the optimum focal position for unit no. 311 is −0.0005 inch. It appears that the curves of Figs. F-2 and F-3 do not behave like the curves of Fig. F-1 or as anticipated in Appendix E. In other words, in Fig. F-2 it was expected that the 0.000 focal position curve would be above the other curves for all IMC mismatches higher than approximately 6 percent. This expectation depended on the apparent low contrast resolution peak being at the

−0.0005-inch focal position. Figs. F-2 and F-3 show that, though for most lenses optimum focus is approximately 0.0005 inch beyond the low contrast resolution peak, this rule is not necessarily true for all lenses. Consequently, the only reliable means of determining the optimum focal position is to perform through-focus resolution tests with various amounts of IMC mismatch for every camera.

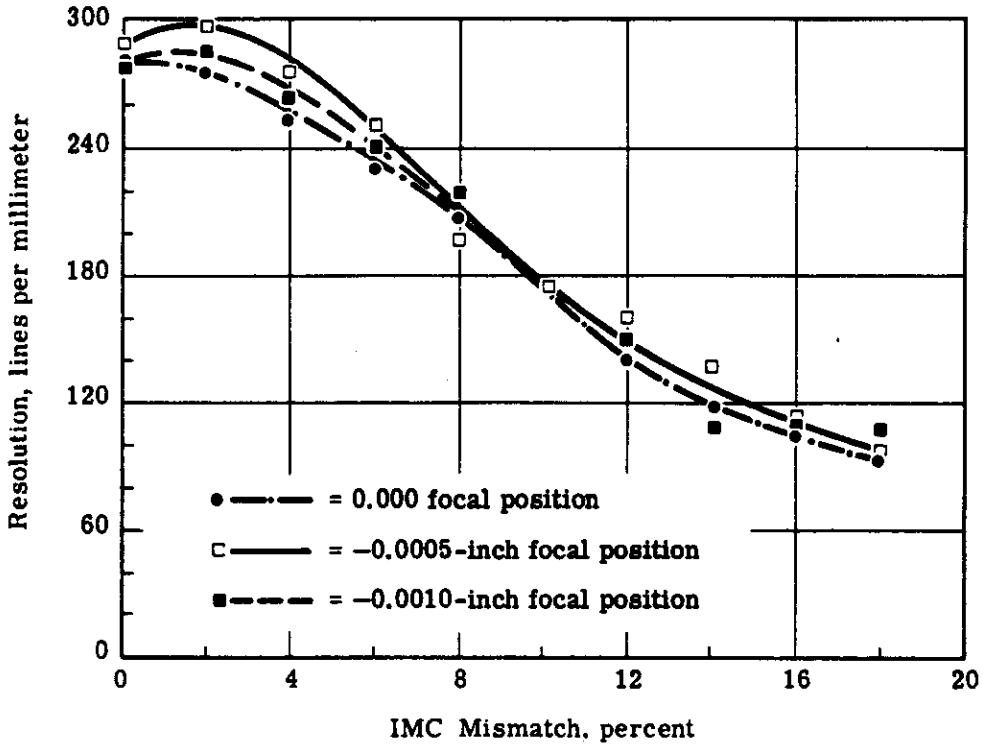

Fig. F-3 — Unit no. 311, high contrast resolution readings